

NASA/CR—2002-211881



Acousto-Ultrasonics to Assess Material and Structural Properties

Harold E. Kautz
Cleveland State University, Cleveland, Ohio

October 2002

The NASA STI Program Office . . . in Profile

Since its founding, NASA has been dedicated to the advancement of aeronautics and space science. The NASA Scientific and Technical Information (STI) Program Office plays a key part in helping NASA maintain this important role.

The NASA STI Program Office is operated by Langley Research Center, the Lead Center for NASA's scientific and technical information. The NASA STI Program Office provides access to the NASA STI Database, the largest collection of aeronautical and space science STI in the world. The Program Office is also NASA's institutional mechanism for disseminating the results of its research and development activities. These results are published by NASA in the NASA STI Report Series, which includes the following report types:

- **TECHNICAL PUBLICATION.** Reports of completed research or a major significant phase of research that present the results of NASA programs and include extensive data or theoretical analysis. Includes compilations of significant scientific and technical data and information deemed to be of continuing reference value. NASA's counterpart of peer-reviewed formal professional papers but has less stringent limitations on manuscript length and extent of graphic presentations.
- **TECHNICAL MEMORANDUM.** Scientific and technical findings that are preliminary or of specialized interest, e.g., quick release reports, working papers, and bibliographies that contain minimal annotation. Does not contain extensive analysis.
- **CONTRACTOR REPORT.** Scientific and technical findings by NASA-sponsored contractors and grantees.

- **CONFERENCE PUBLICATION.** Collected papers from scientific and technical conferences, symposia, seminars, or other meetings sponsored or cosponsored by NASA.
- **SPECIAL PUBLICATION.** Scientific, technical, or historical information from NASA programs, projects, and missions, often concerned with subjects having substantial public interest.
- **TECHNICAL TRANSLATION.** English-language translations of foreign scientific and technical material pertinent to NASA's mission.

Specialized services that complement the STI Program Office's diverse offerings include creating custom thesauri, building customized databases, organizing and publishing research results . . . even providing videos.

For more information about the NASA STI Program Office, see the following:

- Access the NASA STI Program Home Page at <http://www.sti.nasa.gov>
- E-mail your question via the Internet to help@sti.nasa.gov
- Fax your question to the NASA Access Help Desk at 301-621-0134
- Telephone the NASA Access Help Desk at 301-621-0390
- Write to:
NASA Access Help Desk
NASA Center for Aerospace Information
7121 Standard Drive
Hanover, MD 21076

NASA/CR—2002-211881



Acousto-Ultrasonics to Assess Material and Structural Properties

Harold E. Kautz
Cleveland State University, Cleveland, Ohio

Prepared under GSN-002559

National Aeronautics and
Space Administration

Glenn Research Center

October 2002

Available from

NASA Center for Aerospace Information
7121 Standard Drive
Hanover, MD 21076

National Technical Information Service
5285 Port Royal Road
Springfield, VA 22100

Available electronically at <http://gltrs.grc.nasa.gov>

Acousto-Ultrasonics to Assess Material and Structural Properties

Harold E. Kautz
Cleveland State University
Cleveland, Ohio 44115

SUMMARY

This report was created to serve as a manual for applying the Acousto-Ultrasonic NDE method, as practiced at NASA Glenn, to the study of materials and structures for a wide range of applications.

Three state of the art acousto-ultrasonic (A-U) analysis parameters; ultrasonic decay (UD) rate, mean time $\langle t \rangle$ (or skewing factor, “s”), and the centroid of the power spectrum, “ f_c ,” have been studied and applied at GRC for NDE interrogation of various materials and structures of aerospace interest. In addition to this, a unique application of Lamb wave analysis is shown.

An appendix gives a brief overview of Lamb Wave analysis.

This paper presents the analysis employed to calculate these parameters and the development and reasoning behind their use. It also discusses the planning of A-U measurements for materials and structures to be studied. Types of transducer coupling are discussed including contact and non-contact via laser and air. Experimental planning includes matching transducer frequency range to material and geometry of the specimen to be studied.

The effect on results of initially zeroing the DC component of the ultrasonic waveform is compared with not doing so.

A wide range of interrogation problems are addressed via the application of these analysis parameters to real specimens is shown for five cases:

- Case 1: Differences in density in [0] SiC/RBSN ceramic matrix composite.
- Case 2: Effect of tensile fatigue cycling in [± 45] SiC/SiC ceramic matrix composite.
- Case 3: Detecting creep life, and failure, in Udimet 520 Nickel-Based Super Alloy.
- Case 4: Detecting Surface Layer Formation in T-650-35/PMR-15 Polymer Matrix Composites Panels due to Thermal Aging.
- Case 5: Detecting Spin Test Degradation in PMC Flywheels.

Among these cases a wide range of materials and geometries are studied.

INTRODUCTION

Some Background

Acousto-Ultrasonics, (A-U), was invented in the 1970s by Alex Vary as an approach to interrogating materials and structures that presented difficulties to more conventional ultrasonic NDE techniques¹⁻³. A-U employs two transducers. In the earliest concept, the sender was relatively high frequency, say 2.25 MHz, broadband, and the receiver was relatively low, maybe an AE sensor in the 100s of kHz range. The receiving transducer did not directly sense the ultrasound introduced by the sender, but rather sensed the disturbance in the specimen caused by the ultrasound.

A-U was thought of as simulating AE without the associated mechanical stress and possible strain. AE looks for acoustic signatures of stress caused events in the specimen. A-U looked for similar signatures that reveal the mechanical/material condition without changing the specimen by mechanical stress. This would seem to be an improvement over AE if one wishes to assure non-destructivity.

A-U borrowed waveform analysis from AE. Such things as the energy in the waveform, a ring down count, and certain frequency characteristics would be calculated. These things would be determined at the site of the receiving transducer, but having been shaped by the environment the ultrasound experienced in its path from the sending transducer. In A-U one knows where the signal came from, (the site of the sender), and, unless the sender is decoupled and recoupled, one knows that the input signal strength is a constant. For AE the signal can come from many places in the specimen and the strength is one of the signature variables.

The term: “stress wave factor” (SWF), came from AE. It can have several forms. It is used as the name of the analysis variable under consideration. In AE it refers to the fact that the wave is due to a stress. In A-U it refers to a wave that simulates the effect of a stress.

The SWF is taken as a measure of the ability of the specimen to transmit the ultrasound from its site of origin to site of detection. A concern of those who design materials and structures is to design-in the ability to dissipate stresses, (as, for example, with hardware in service), in a harmless way. If the A-U signal simulates a wave due to stress then the SWF should indicate how strong a signal survives the journey from sender to receiver. We have two properties of ultrasound to work with: velocity, and attenuation. These are measures of this ability to transmit ultrasound.

In AE one generally must work around velocity and attenuation to get at the signature of the event site. In A-U one uses these properties. Changes in velocity signify changes in stiffness. Changes in attenuation can be caused by changes in material properties like porosity, crack formation, or other disordering that can be caused by thermomechanical treatment.

Evolution of A-U

An early change was to match the frequency of the two transducers. One chooses a frequency range of interest. In order to maximize precision one makes that range a large part of the signal sent and received. And so the receiver is made to be most sensitive to the frequency range that the sender produces.

Reproducibility is an important consideration for A-U. The greatest sensitivity is in the magnitude of the collected signal. A major problem is coupling reproducibility for both the sender and receiver. For the sender, we don't really know how much signal strength gets into the specimen from time to time or place to place. For the receiver the problem is ambiguity as to the amount of signal reflected back into the specimen. For contact transducers there can be differences, for example, in surface roughness or coupling pressure. For air coupling and lasers there is variability of reflection at the specimen-air interface.

Transducer decoupling and recoupling is necessary in many applications. In some programs one would like to follow the progress of thermomechanical cycling and, one might hope to learn to predict life. In other programs one would like to compare the state of health at different positions on a panel or maybe around a rotor. In various cases it is necessary to be able to make confident comparisons between different cycles or positions.

For this reason we look for measurement parameters that are independent of coupling. This would give us independence from signal magnitude. Thus we seek variables that are dependent only on the shape of the waveform in time or frequency. An example of this is to determine ultrasonic velocity from geometric considerations and arrival times of pulses.

Velocity cannot always be determined with enough precision in the A-U configuration and otherwise has been of less interest than attenuation. An exception to this is the work of Tang and Henneke at VPI⁴. They developed a method to determine Lamb Wave velocities and calculate stiffness moduli for plate like geometries. This is useful for nondestructive study of coupons that are typical of the types commonly employed in development of materials.⁵ An important requirement is to be working with specimens of plate like geometry.

We cannot get directly at attenuation with A-U. But we can get at time rate of signal decay through the shape of the waveform. The earliest version of this was ring down count. For this the decay of a fairly narrow band signal, (the ring down) is followed. The number of voltage excursions greater than a chosen threshold were counted. With the advent of digital waveform analysis this was superseded by diffuse field decay.^{6,7}

For diffuse field decay one designs a specimen-frequency combination that causes the received waveform to be totally diffuse. This means that the identity of individual wave paths is lost. The receiving transducer simply sees an ultrasonic energy flux which decays with time. The references do not express the condition in terms of a

wavelength—dimensions relationship. Weaver,⁶ states (p. 427): “The ultrasonic field is allowed to distribute itself diffusely across the specimen.” This implies that the receiving transducer intercepts wave paths from a wide distribution of directions and places of reflection. Lott et al.⁷ states (p. 1): “The analysis is based upon the premise that a diffuse ultrasonic field in an isolated sample will decay only from internal absorption mechanisms when external damping by air and fixturing is minimal.” Under these experimental conditions the shape of the waveform in time mimics the exponential decay that the ultrasonic signal experiences over distance. The decay constant with distance is the attenuation coefficient and is considered a fundamental property of ultrasound. If one were dealing with a nondispersive signal, then the velocity would be constant and could be used to calculate an attenuation coefficient from the diffuse field decay constant. However, in most A-U situations one has dispersion and the velocity is not well defined.

ANALYSIS TECHNIQUES

Present day A-U measurements

Not only is the velocity not well defined, but in many applications we also do not have the luxury of designing a specimen that yields a true diffuse field. What this means in terms of the preceding quote from reference 7 is that “external damping by air and fixturing is *not* minimal.” So it is often necessary to compromise and calculate an ultrasonic decay (UD) rate. Experimentally, we try to assure that the external damping is a constant from one measurement to another. Then comparing the results will reveal differences in internal absorption. The philosophy of UD rate is that, after all, the signal is decaying away exponentially. We may not have a perfect exponential decay but we can treat it that way and do a linear regression of the log signal variable against decay time. The important thing is to use the same experimental parameters for all the measurements in a given project from one cycle or position to the next.

In addition to the UD rate we consider two other parameters: a waveform mean time (or alternately a skewing factor), which is another approach to measuring the signal decay with time, and the centroid of the power spectrum, which is a different approach to analyzing the effect of specimen properties on the frequency spectrum of the applied signal.

Another important form of A-U analysis is the determination of Lamb wave velocities by the approximate theory, developed by Tang and Henneke, referred to earlier.⁴ That analysis technique will not be detailed here. (However, for the sake of completeness a brief description is provided in an appendix.)

A-U waveforms are generally long in the time domain. The actual length of the time record depends upon the attenuation and geometry of the specimen being studied as well as the frequency range applied by the transducers. For CMC or MMC tensile fatigue specimens of the geometry we typically study we use 1 to 2.25 MHz broadband transducers and collect waveform records a few hundred microseconds in length. If we have lower frequency transducers or lower attenuation we go to longer time records

because the signal decay is slower. Of course for higher frequency or higher attenuation the record can be shorter. The final decision depends upon looking at a waveform and making a judgment. The waveforms are the superposition of many pulse arrivals that have followed many paths from sender to receiver and arrive there at different times. This condition encourages time domain partitioning which is necessary for calculating decay rates, and is also useful for examining different segments of the signal separately. It is likely, for example, that later segments in the waveform contain pulse arrivals that have sampled regions of the specimen that are farther from the most direct sender to receiver path than are earlier segments. Each time domain segment can be Fourier transformed to allow us to frequency filter it. So in fact we often slice up a waveform in two dimensions, time and frequency.

The UD rate

Since it is related to the attenuation coefficient, $\alpha(f)$, the UD rate coefficient, $\beta(f)$, is also dependent on frequency. An important difference between them is that, while $\alpha(f)$ has units of Np/distance, $\beta(f)$ has units of Np/time. If $\beta(f)$ were constant with frequency it could be determined directly from the time domain A-U waveform $\varphi(t)$. In order to determine the energy dissipation one would use, not $\varphi(t)$, but $|\varphi(t)|^2$:

$$|\varphi(t)|^2 = K \text{Exp}(-\beta t).$$

[$|\varphi(t)|^2$ is the energy density of the waveform and is a positive definite function that looks much like the plus half of the A-U waveform. Note that the β is two times what we would get if we use the first power of the A-U waveform.]

As we indicated earlier, β is not a constant in this equation, but rather a function of frequency. For this reason we must express the frequency dependence of the A-U waveform:

$$|\varphi(f,t)|^2 = K(f) \text{Exp}(-\beta(f)t)$$

and we also acknowledge that the pre-exponential factor, $K(f)$, may also depend on frequency, but not time. This factor is the energy at frequency f inputted at the sending transducer diminished by factors, such as the losses due to coupling at the transducers, and any other factors that are time independent.

It is desirable to Fourier transform the waveform $\varphi(f,t)$ to the frequency domain and work with the power spectrum, PS. The above equation expresses the energy density in the waveform at a particular time, t , and frequency, f . The power spectrum at a given time and frequency, $\text{PS}(f, t)$, is the same energy density as $|\varphi(f,t)|^2$, so:

$$\text{PS}(f, t) = K(f) \text{Exp}(-\beta(f)t).$$

$\beta(f)$ can be determined as the slope in a log regression of this function in the time domain. The practical way to do this with digitally encoded waveforms is to calculate the

power spectrum for time partitions (t_1, t_2) . The power spectrum, is itself digitally encoded. If we integrate over frequency we get the zero moment, M_0 of the power spectrum of this time interval. We assign this to a time t_{part} where:

$$t_1 \leq t_{part} \leq t_2.$$

A good way to do this is to choose a set of time partitions where $t_2 - t_1$ is always the same length, and then choose t_{part} as the center of each individual partition.

$$M_0(t_{part}, f_1, f_2) = \int_{f_1}^{f_2} K(f) \text{Exp}(-\beta(f)t_{part}) df$$

We approximate the UD rate as a constant, $\beta(f_{filt})$, for the frequency range (f_1, f_2) . It is exact for some frequency:

$$f_1 \leq f_{filt} \leq f_2.$$

[This double inequality is true as long as the UD rate coefficient, $\beta(f)$, is a continuous, monotonic function of frequency. This is likely always so.] In any case one should always report results in terms of the interval, (f_1, f_2) , which is something we know for sure.

Using the frequency f_{filt} simplifies the expression for the zero moment to:

$$M_0(t_{part}, f_{filt}) = \text{Exp}(-\beta(f_{filt}) t_{part}) \left[\int_{f_1}^{f_2} K(f) df \right]$$

The integral over $K(f)$ is independent of (and therefore a constant of) time. If we do a logarithmic regression of $M_0(t_{part}, f_{filt})$ against t_{part} for a range of time partitions in the A-U waveform the slope will be $-\beta(f_{filt})$, and we report β as the UD rate for the interval (f_1, f_2) .

There may be occasions when one would like to determine UD rate as a function of frequency. In this case one would calculate β for several sets of filters (f_1, f_2) . Then it would be useful to present the results in terms of an f_{filt} , probably taken as the center of the filter. This calculation employs a frequency interval for the power spectrum, PS (f_1, f_2) , of the A-U time domain waveform, $\varphi(t)$. $\beta(f_{filt})$ is taken as representing the UD rate for the frequency interval (f_1, f_2) . If one calculates $\beta(f_{filt})$ for different frequency intervals one gets different $\beta(f_{filt})$ values. Because of its relationship to ultrasonic attenuation one expects higher $\beta(f_{filt})$ values at higher ranging frequency intervals.

The frequencies f_1 and f_2 are chosen to match the frequency spectrum of the received signal and to exclude noise. The width of the frequency filter, $f_2 - f_1$, is a compromise. Wider filters give more precise $M_0(t_{part}, f_{filt})$ but the log plot is less linear. Narrower filters give the reverse. From the set of time intervals, (t_1, t_2) , a range is chosen which is as close to linear as possible for the zero moments, $\log[M_0(t_{part}, f_{filt})]$. It is desirable that the intervals, (t_1, t_2) , be the same for all iterations of measurements for successive cycles

or positions in the experiment. (This last condition can require some judicious planning of experimental parameters at the beginning.)

Mean time and Skewing factor

An A-U waveform typically is composed of an initial dead time before the first signal pulse arrives at the receiver, a rise portion often dominated by early plate modes,⁴ the exponential decay portion for which we determine $\beta(f_{\text{filt}})$, and finally a region where the decay signal becomes small compared to noise. Conditions may exist such that the exponential decay portion is difficult to separate from the rest of the signal. It may be that we can observe qualitatively that a signal from one specimen state extinguishes faster than from another specimen state, but we do not have confidence in contrasting their $\beta(f_{\text{filt}})$ values.

If this is so one might resort to a mean time of the waveform, which takes advantage of the fact that the decaying A-U signal has magnitude that is weighted towards the earlier part of the signal.

We define a mean time $\langle t \rangle$, of the waveform $\varphi(t, f_{\text{filt}})$ for the interval (t_a, t_b) as:

$$\langle t \rangle = \frac{\int_{t_a}^{t_b} |\varphi(t, f_{\text{filt}})|^2 t dt}{\int_{t_a}^{t_b} |\varphi(t, f_{\text{filt}})|^2 dt}$$

Here $|\varphi(t, f_{\text{filt}})|^2$ is the square of the absolute magnitude of the original waveform after it has been filtered for the frequency range of interest. (We choose to use the square of the filtered waveform $\varphi(t, f_{\text{filt}})$ in order that we obtain a mean time, $\langle t \rangle$, of the energy in the signal which is a similar consideration as with the UD rate.)

[Note that the time interval here, (t_a, t_b) is not the same as the partitions, (t_1, t_2) used in the UD rate calculation. There will be only one time interval here. If we are interested in simulating the same conditions as in the UD rate calculation t_a might be chosen as the earliest t_{part} used above and t_b the last. But this is not necessarily so. The frequency filter f_{filt} does have the same meaning as with UD rate.]

The mean time will behave opposite to the UD rate. That is, for increasing UD rate the mean time will decrease.

We can define a skewing factor, s , as:

$$s = [(t_a + t_b)/2 - \langle t \rangle] / (t_b - t_a)/2$$

The properties of s are that it varies between 1 and -1 . When s is greater than zero the waveform $\varphi(t, f_{\text{filt}})$ is skewed toward the beginning of the time interval, as with an exponentially decaying signal. We expect that s will be larger, but $\langle t \rangle$ will be smaller, with larger UD rate coefficient, but their precision does not depend on the presence of an exponential decay in the signal.

In some applications it may be better to compare skewing factors but for the examples in this study the mean time, $\langle t \rangle$, is easier to discuss.

Centroid of the Power spectrum

The centroid, f_c is a different approach to A-U signal analysis but is also obtained from the power spectrum. It is part of the general method of moments which has already been applied to A-U.⁹ We can, again, choose an interval (t_a, t_b) in the time domain waveform and determine its magnitude spectrum. The power spectrum is, point by point, the square of the magnitude spectrum. So we have a power spectrum $PS(f, t_a, t_b)$. The centroid is

$$f_c (f_1, f_2, t_a, t_b) = \int_{f_1}^{f_2} PS (f, t_a, t_b) f df / \int_{f_1}^{f_2} PS (f, t_a, t_b) df$$

The integral:

$$\int_{f_1}^{f_2} PS (f, t_a, t_b) df = M0(f_1, f_2, t_a, t_b)$$

Is called the zero moment of the power spectrum and the integral:

$$\int_{f_1}^{f_2} PS (f, t_a, t_b) f df = M1(f_1, f_2, t_a, t_b)$$

is called the first moment. We can express the centroid as:

$$f_c (f_1, f_2, t_a, t_b) = M1/M0$$

One can define an n^{th} moment M_n as⁹:

$$\int_{f_1}^{f_2} PS (f, t_a, t_b) f^n df = M_n(f_1, f_2, t_a, t_b)$$

as well as higher order mean frequencies. The moments are less desirable for our work because they are subject to errors due to signal magnitude variations from measurement to measurement. The frequencies are not so subject. If one uses mean frequencies that are higher order than f_c the results are more sensitive to the high frequency portion of the signal.¹⁰ This may or may not be desirable.

The application of the A-U analysis parameters to real situations.

Type of transducer coupling.

There are Gels that can be placed between the specimen surface and the transducers' wear plates. At this laboratory we have used Ultragel-II by Echo Ultrasonics and Couplant D by Panasonics. They appear to work equally well. The primary consideration is that they not significantly add to or subtract from the ultrasonic signal passing through them. They should wet well the surfaces they touch. Generally they are water based for easy clean up. Nonetheless the application and clean up can be inconvenient. Of course if water, or whatever the solvent, attacks the specimen surface one cannot use the gel. One cannot use a gel if the specimen is porous. We have experienced an effect with 30 per cent porous SiC/RBSN ceramic composites measured employing a gel couplant. The A-U signal from a second time measurement is different from the first time. Only after

washing the specimen and heating to bring the weight back to equilibrium did the A-U signal return to normal.

One might consider doing A-U in an immersion tank. The leaky Lamb Wave technique employs this configuration. Here the Lamb wave equations of Tang and Henneke⁴ must be modified. We cannot approximate the specimen faces as infinite reflecting planes. Ultrasound may be introduced at a single sender site, but it radiates out everywhere. The acoustic impedance difference between the specimen and liquid is much less than with air. Ultrasonic Decay is less interested in the boundary condition than the fact that much energy is lost before reaching the receiver position.

At this laboratory we have made much use of elastic dry couplant pads. The motivation for this is to avoid the disadvantage discussed for gel couplants. An added advantage here is that the pad can be shaped differently from the transducer wear plate. This can allow better definition of the point of entry and exit of the A-U signal. A disadvantage is that the pads attenuate a lot of signal. We find we cannot use pads above about 5 MHz. Of course the thinner the pad the less the attenuation. We make pads from a white silicone adhesive/sealant with the brand name RTV. We make them the thickness of a microscope slide. (Cementing them to the wear plate with the same RTV adds to the thickness.)

The elastic pads really have three effects on the A-U signal; they decrease the magnitude, change the spectrum shape of the signal, and they add a time delay. These effects are sensitive to the force with which the transducers are pressed to the specimen surface. We have standardized on 10 lbs total for the two transducers. The effect of varying the force has been studied.¹¹ The choice between gel and elastic pad coupling for a given experiment depends upon the advantages and disadvantages mentioned above. However, when doing a comparison study between specimens or specimen states it is necessary to remain with the original choice of couplant.

Non-contact A-U can be done with lasers or air coupled transducers. Laser-in (the sender) should be discussed separately from laser-out (the receiver).

Laser-in involves the absorption of the electromagnetic energy at the specimen, conversion to thermal energy, and thermal expansion conversion to acoustic energy. The mechanism for this depends upon the material of the specimen. In some cases the specimen material will absorb the laser energy near the surface. We have experimental evidence that SiC/Ti 6-4 metal matrix composites absorb the laser energy by vaporization of surface material such as water. In this case there can be a loss of sensitivity after initial laser pulsing until the layer reestablishes. In both these cases the ultrasound appears in the specimen at the surface. This leads to the establishment of propagation paths similar to those with contact transducers.

We have found that absorption of laser energy with polymer resins is different.¹² A PMR-15 neat resin panel as thick as 0.586 cm absorbs the 1.064 μm NdYAG pulse and still transmits a significant amount out the back surface. This means that the ultrasonic energy

appears in the interior of the panel rather than at the surface. This may lead to different wave modes propagating than with contact transducers.

One might expect that a polymer resin would have less tolerance to a laser pulse destructive power than other high temperature materials we study. Whereas the SiC/Ti 6-4 MMC as well as the CMCs we studied showed no permanent damage up to 60 mJoules, the PMR-15 began decomposing for energy greater than 5.6 mJoules.¹² Carbon fiber reinforced PMR-15 shows damage as low as at 6 mJoules. Principally, the carbon fibers are burned away and the laser pulse is stopped very quickly.

Another difference between materials is surface reflectivity. Certainly a metallic surface will reflect back more laser energy than, for example, a rough ceramic.

Laser-out involves the use of some sort of laser interferometer to sense specimen surface displacements caused by ultrasound emerging from the interior. A Doppler shift device seems the most workable. Even so, we have had great difficulty attaining adequate optical alignment. Our experience with several systems is that the signal to noise ratio is not acceptable above a few hundred kHz.

Air-in and air out can be discussed together. There are three barriers to doing this successfully; a large solid to air acoustic impedance mismatch, attenuation in air, and a large air to solid acoustic impedance mismatch. It turns out that attenuation in air is not a serious problem. The solid – air interfaces are the greatest causes of signal strength loss. Air in is the worse case. We have not been able to receive an air sent A-U signal with any type of transducer coupling. Air-in has had some success claimed for through transmission ultrasonics, and it has been successful using front surface reflections,¹³ but not in the A-U configuration. However we have been successful in using air-coupled transducers up to 0.5 MHz as receivers for laser or contact sent signals.

The one successful totally non-contact configuration has been laser-in and air-out^{11,14}

One must keep in mind that the velocity of sound in air is about 340 m/sec.¹⁵ This adds a delay of about 74.71 μ seconds to the signal arrival time for every inch of air gap. If we are not aware of this we might look for the A-U waveform in the wrong time region. Also, because of this reason it is unlikely that we would want to collect waveforms without a trigger delay.

Specimen support.

A study has been made on the effect of various support structure geometries on the sensitivity of UD rate measurements to changes in material/mechanical properties.¹¹ That report addresses the fact that many different sources of signal loss can contribute to the exponential ultrasonic decay that is observed. The strength of the output signal at the receiving transducer can be expressed as the input strength at the sender multiplied by many factors. Some may be exponential in time some may not. Only the ones that are exponential affect the observed ultrasonic decay rate. The observed $\beta(f)$ can be expressed as:

$$\beta(\mathbf{f}) = \Sigma \beta_i(\mathbf{f}).$$

Only one of the $\beta_i(\mathbf{f})$'s is likely to be due to the material properties. Ultrasonic decay, like most A-U, depends on comparing measurements from before to after some change. One seeks to determine $\Delta\beta(\mathbf{f})$ where:

$$\beta(\mathbf{f})_{\text{after}} - \beta(\mathbf{f})_{\text{before}} = \Delta\beta(\mathbf{f})$$

In the cited study $\Delta\beta(\mathbf{f})$ is made to be differences in type of support for the specimen, whether the support be a rubber pad, a set of wood sticks, or something else. The result was that this $\Delta\beta(\mathbf{f})$ can be quite sizable. So it turned out that, whenever possible, the specimen under investigation ought to be supported minimally as with the wood sticks.

The above seems to imply that $\Delta\beta(\mathbf{f})$ loss to air is quite small compared to other losses. This is true, and it point out a problem with air coupled non-contact A-U. The strength of the received signal depends on this quite small leakage to air, which we consider neglectible in contact A-U.

Sometimes we may not have the option to minimize support structure. An example may be to examine a blade attached to a rotor. Here there may be losses to the support structure that cannot be eliminated. The cited study shows that there is hope that we can detect changes in blade $\Delta\beta(\mathbf{f})$ provided the other losses don't change from before to after.

Choice of frequency range.

A first consideration may be choice of ultrasonic transducer frequency. We earlier referred to an approximate theory developed for Lamb wave analysis in composite plates.⁴ From this report it can be seen that the type of A-U waveform recovered depends strongly on the ratio:

$$\lambda/h = V/fh$$

λ is the wavelength of the ultrasound and h is the specimen thickness in the direction normal to the transducer face. More readily accessible experimental quantities are shown on the right. V is the wave longitudinal velocity in the material, which is easier to, at least estimate, than the wavelength. f is the frequency that is applied. It has been shown,¹⁶ that for λ/h large, very coherent lowest-symmetric and lowest-antisymmetric Lamb wave pulses can be collected. For λ/h small, higher order, generally dispersive, waves are collected. This latter condition is the diffuse field regime. For this reason we would like to make UD measurements at as high a frequency as practical. The main limitation to this is the increase of attenuation with frequency. We have to work at low enough frequency so that we can recover a useful signal. UD measurements are often done in a compromise frequency regime that has λ/h between the Lamb wave and Diffuse field limits. A useful reference frequency is that for through thickness resonance of the fundamental frequency:

$$V/fh = 2.$$

If a frequency is chosen such that:

$$V/fh > 2,$$

Then the wavelength is greater than the thickness, the ultrasound propagates similar to in a waveguide, and the lowest Lamb Waves are very important.

It would be good if one can do ultrasonic decay in a range of frequencies, f , such that:

$$V/fh < 2,$$

Here the wavelength is less than the thickness and the higher, more disperse, modes become important. The greater this last inequality, the more the ultrasound becomes like a diffuse field.

Another consideration is the length of the signal record. An A-U signal typically starts with a rise in amplitude and then the decay into noise. It is good to collect a long enough record to capture much of that decay but not waste too much at the end on noise. We would like a waveform such that a plot of $\log M_0(t_{\text{part}}, f_{\text{filt}})$ vs t_{part} has a significant range of linearity.

RESULTS

Comparison of the three waveform analysis parameters for assessing material and mechanical properties.

We compare them in five experimental cases. In case 1 we will begin by demonstrating the effect of the choice of transducer frequency range on the type of A-U signal that one collects. We will also examine the effect of zeroing the DC component of the collected signals before performing the calculation of the analysis parameters.

Case 1: Differences in density in [0] SiC/RBSN ceramic matrix composite.

Specimen 19 has a fully densified silicon nitride matrix whereas specimen 99 has 30 percent matrix porosity. Otherwise they are identical. We expect that scattering at pores will cause ultrasonic attenuation in the less dense to be greater from what it is in the fully dense specimen.

Effect of transducer frequency range:

As an example of the effect of frequency on the A-U waveform, figure 1 compares waveforms on specimen 19 that were collected in different ranges. With specimen thickness, $h = 0.22$ cm and velocity, $V = 0.8$ cm/ μ second,¹⁷ we have:

Figure 1a shows the 2.25 MHz data where, for the center frequency, $V/fh = 1.62$, figure 1b shows 1.0 MHz data where $V/fh = 3.65$, and figure 1c shows 0.5 MHz data where $V/fh = 7.3$.

As the ratio is increased the discrete Lamb wave pulses become more pronounced. Finally at 0.5 MHz they dominate the waveform. The lowest symmetric Lamb mode is the first pulse arriving at the receiver, and is at about 10 μ seconds into the record. The larger antisymmetric pulse arrives at about 27 μ seconds into the record. One could calculate an exponential decay rate from any of these waveforms. However, at least for the 0.5 MHz data, the rest of the record is made up predominantly of Lamb wave reflections from edges. These are affected by geometrical properties rather than material. The condition shown in figure 1a, with 2.25 MHz transducers is well within the ultrasonic decay region.

Figure 2 shows the 2.25 MHz waveforms collected on the two specimens of different density. The same time, frequency, and geometrical conditions were used to collect these data. The 2.25 MHz broadband transducers were coupled through dry couplant pads at approximately 3.2 cm separation on the same side of the specimen. 200 microsecond records were collected at 25.0 MHz sampling rate. Visual inspection of these data in figures 2a and 2b shows clearly, though qualitatively, that specimen 99 has higher decay rate than does 19. This is in agreement with the knowledge that specimen 99 has matrix porosity that is not present in specimen 19. In order to obtain quantitative information the waveform data must be analyzed.

Figures 2c and 2d show the 5 to 7.3 microsecond portions of the signal. The lowest symmetric plate wave pulse always arrives first. If we examine the central “dip” of this pulses we see that the specimen 19 arrives earlier, at about 6.69 microseconds, and the specimen 99 arrives later, at about 6.76 microseconds. This is in agreement with earlier work¹⁷ where it was shown that this plate mode velocity increases with density in this SiC/RBSN material. In order to make more precise measurements of these velocities, as well as for the lowest antisymmetric mode, it is best to work at lower frequency, as in figure 1c, use a higher sampling rate, and regress arrival times over several transducer separation values.

Effect of zeroing the DC component of the collected signals.

The analysis starts with inspection of the magnitude spectra in figure 3. There are differences in the spectra of the two specimens. Specimen 19 in figure 3a exhibits a large magnitudes in the range of about 1.75 to 2.75 MHz. Specimen 99 in figure 3b exhibits smaller magnitude broader width signal. There is significant magnitude in other ranges, especially very low frequency, which we treat as unwanted noise. We chose to do our analysis for the frequency filter range of 1.75 to 2.75 MHz. Figures 3c and 3d show magnitude spectra from the same data as figures 3a and 3b respectively but determined after the original waveforms were DC zeroed. (That is, the mean of the total time domain signal is set equal to zero.) Comparing figure 3c to 3a and 3d to 3b one sees that, not only the $f = 0$ values, but also a range of values for $f > 0$ are different. Still, it does not seem from this that analysis parameters for 1.75 to 2.75 MHz should be significantly altered by eliminating the DC. However, it would seem to be a good practice to eliminate the DC since its presence is an experimental error.

UD rates are determined from the linear regression of the natural log of power spectrum integrals versus time. Figure 4 shows plots of the integral of power spectra from 1.75 to 2.75 MHz with 12.5 microsecond partitions of $\phi(t)$.

The classic A-U waveform, $\phi(t)$, displays an initial rise followed by an exponential decay into background. Figure 2 showed that $\phi(t)$ for each of these specimens had this behavior. Between these end regions of the waveform one hopes to encounter an exponential decay region. An exponential region will appear in the semi-log plot, figures 4, as linear. It is fairly straight forward that such a region starts after the first 12.5 microsecond partition. It is much less straight forward where to end a regression to avoid background interference and obtain a good UD rate. Figures 4c and 4d are results from the same waveforms as figures 4a and 4b respectively. Only with the later two the waveforms have been DC zeroed. Although specimen 19 in 4c does not appear greatly changed from 4a, specimen 99 in 4d looks quite different from 4b. The DC zeroing has lengthened the linear portion of the curve. What has also happened, however, is that subtracting the DC from the original waveform has cause increase in scatter error in the last four partitions due to the smallness of the original signal there. For these data points the original signal has decayed enough to be comparable in magnitude to the DC.

Figure 5 shows the results of doing linear regressions for each specimen from 25 microseconds out to various end times. In figure 5a the UD rate regressions are calculated without DC zeroing. Specimen 19 shows no significant difference in slope for the entire range from 25 to 200 microseconds. In the case of specimen 99, the shorter the interval from 25 microsecond the greater the slope. It is difficult to choose a proper UD rate in specimen 99 for comparing to specimen 19.

In figure 5b the specimens are compared from data using DC zeroed waveforms. Here they are more easily distinguished.

Figure 6 shows the mean times, $\langle t \rangle$, for the two specimens. No difference in $\langle t \rangle$ values was found whether the waveforms were DC zeroed or not. We use only DC zeroing in this figure. These are calculated for the intervals 0 to 200, 0 to 150, 0 to 100, and 0 to 50 μ seconds. This parameter distinguishes, very well, the difference in $\langle t \rangle$ between the specimens. Except for 0 to 50 μ seconds on specimen 19, the $\langle t \rangle$ value is nearly insensitive to the range over which the mean time is calculated. Figure 2a shows that the 0 to 50 μ seconds calculation leaves out a large portion of important signal. Figure 6 shows that the mean time is a good parameter when the A-U waveform does not have a sufficiently log-linear segment to obtain a good UD rate. The fact that specimen 19 has smaller $\langle t \rangle$ values means that its A-U waveform, $\phi(t)$, is concentrated more towards the early portion than is the waveform of specimen 99 over the same time segment. This is in agreement with the condition that specimen 19 has the faster ultrasonic decay.

Figure 7 displays the centroid of the power spectrum, f_c , for specimens 19 and 99. These were calculated using DC zeroed waveforms. (Calculations with DC zeroed waveforms were compared to calculations with non-zeroed and no significant differences were found.) The f_c values are calculated for four, 50 μ seconds segments for the filter 1.0 to

3.0 MHz. Each f_c is plotted in figure 7 at the center of its segment. The filter, wider than with the UD rate calculation, is chosen to express the difference in the power spectra of figure 3. The decrease at longer times probably reflects the greater influence of background at longer times because of the smaller signal.

Specimen 99 has lower f_c than specimen 19. This would be expected with higher attenuation due to porosity. (Attenuation increases are expected to be more pronounced at higher frequency), The calculated 1 to 3 MHz centroid for the total waveform, (0 to 200 μ seconds), is for specimen 19 = 2.0025 ± 0.0416 , for specimen 99 = 1.8051 ± 0.0616 MHz. These values, not shown, agree well with the value for the 0 to 50 μ seconds segment.

Case 2: Effect of tensile fatigue cycling in [± 45] SiC/SiC ceramic matrix composite. Specimen 32 is measured in the “as fabricated” state and specimen 28 has 10,000 cycles to 10 ksi. Their time domain waveforms, $\phi(t)$, are shown in figure 8.

In specimen 28 we look for the effect of cycling induced matrix cracking that is not present in specimen 32. The matrix cracking is expected to increase ultrasonic attenuation and therefore add a factor to the UD rate. Comparing these two specimens is a good simulation of before and after fatigue cycling. Results with this material have been reported.¹¹

The same time, frequency, and geometrical conditions were used to collect data on both specimens. 2.25 MHz broadband transducers were coupled through dry couplant pads at approximately 3.2 cm separation on the same side. 400 microsecond records were collected at 12.5 MHz sampling rate. For these specimens $V \sim 0.8$ cm/ μ seconds, and $h = 0.27$ cm. Therefore at the transducer center frequency of 2.25 MHz

$$V/fh = 1.32.$$

Figures 8 through 13 show the same types of information as figures 2 through 7 do for the SiC/RBSN. (A all these results were determined using DC zeroed waveforms.)

Figure 8 shows quantitatively the effect of the fatigue cycling on no. 28 when compared to no. 32. The no. 28 signal decays into background more rapidly than does no. 32. In addition, the initial rise in the no. 32 signal is realized at about 15 microseconds into the record. For specimen 28 this does not occur until about 20 microseconds. This is similar to the effect observed in case 1, figures 2c and 2d. The relative lateness of no.28 may signify loss of stiffness and hence lower ultrasonic velocity due to the fatigue cycling. [The “time dilation” of the no. 28 due to velocity degradation could affect the observed UD rate. This might have to be considered when comparing the two specimens.] We will start the UD rate regressions no earlier than 20 microseconds for each specimen. [Of course, in real life, choices for analysis of the “before” data cannot be based on the condition of the “after” state until fatigue cycling is finished. But as long as we have retained the waveform files we can recalculate all data on the same basis at the end.]

Figure 9 shows the frequency magnitude spectra for specimens 32 and 28. This data reflects the choice of transducer frequency range. The analysis will be carried out on the 1.4 to 2.4 MHz filter of the signal. [One might argue that the V/fh calculation for 2.25 MHz is not appropriate for this data. But even if we use $f = 1.75$ MHz the ratio is 1.69 which is still below the resonance condition.]

Figure 10 shows plots of the integral of power spectra from 1.4 to 2.4 MHz for 10 microsecond partitions of $\varphi(t)$. Both of these plots are fairly linear from 20 out to about 200 microseconds. Specimen 28 in figure 10b will turn out to have higher UD rate and thus the signal decays into noise at about 250 microseconds. (This specimen shows the same effect, after 250 microseconds, due to waveform DC zeroing as did specimen 99, after 150 microseconds, in figure 4d. A value of DC zeroing may be that it shows where the signal has decayed to the noise level.)

Figure 11 shows the results of doing linear regressions for each specimen from 20 microseconds out to various end times. The 20 to 200 microsecond results seem good for comparing these specimens. We know that the fatigued specimen 28 waveforms have decayed out of the useful range by 250 microseconds. The 20 to 100 microsecond point for specimen 28 has large scatter. That leaves 20 to 150 and 20 to 200 for comparing the specimens. Either point shows a clear difference between the fatigued and unfatigued specimens.

Figure 12 shows the mean time $\langle t \rangle$ for the two specimens. Mean time is calculated for 0 to 400, 0 to 300, 0 to 200, and 0 to 100 μ second segments. Results are similar to the case 1, figure 6. The fatigued specimen 28 has the lower $\langle t \rangle$ and is relatively constant for all the segments. The specimen 32 values decrease with earlier times due to the fact that significant portions of the signal are left out of the mean. As with UD rate, the $\langle t \rangle$ values exhibit a difference between non-fatigued and fatigued state. Either parameter could be used to monitor the conditions in this material.

Figure 13 compares the 1.4 to 2.4 MHz centroid of the power spectrum for specimens 32 and 28 for 100 microsecond segments out to 400 μ seconds. The f_c values are plotted at the centers of the appropriate segments as they were in case 1. There is not a statistically significant difference between the values for fatigued and the unfatigued specimen when compared using f_c .

Case 3: Detecting creep life, and failure, in Udimet 520 Nickel-Based Super Alloy.¹⁸

This is an experiment in which we wish to compare conditions at different positions on the same specimen. We wish to identify the location of failure, which is between the 0.5 and 0.75 inch measurement positions. The specimen was designed, by means of varying its width, so as to have, nominally, regions of 100, 50, 25, and 12.5 per cent used up creep life. We would like also to be able to differentiate between these regions.

Since the specimen positions are only 0.25 inches apart we want to take care to see only an A-U signal typical of the position of measurement and not a mixture with adjacent positions. This means the ultrasonic wave paths from sender to receiver should not

wander too far. [This is quite at odds with the concept of a “diffuse field.” But we will continue anyway.]

We use a 2.25 MHz dual element transducer pair with a gel couplant. (Elastic pad coupling is not acceptable because the close proximity of sending to receiving element would lead to the presence in the output signal of reflections totally within the pads. This might be true even if one could effectively separate the sender pad from the receiver pad.) This geometry promotes the condition that the sender to receiver path be dominated by waves that do not wander too far. The frequency 2.25 MHz, the thickness of 0.4 cm, and ultrasonic velocity of ~ 0.6 cm/ μ second combine to give:

$$V/fh \sim 0.67.$$

One could use a higher transducer frequency to attenuate long wave paths but the present range is chosen as a compromise to assure strong signal strength. We use a 7 microsecond delay as dictated by the experimentally observed delay line effect in the dual element unit and then a 10 microsecond waveform record length. The very short waveform record length is used to minimize wave paths that stray to other positions on the specimen.

In the more conventional configuration the sender and receiver are farther apart. In cases 1 and 2 the separation was 3.4 cm. The receiver collects a signal that has gone through many reflections and undergone many mode changes. In the present case the sender and receiver are within 0.6 cm of each other. (This estimate of the separation is based on the centers of two semicircular wear plates being close together along their diameter lines.) Under these conditions the signal is practically a pulse echo, dominated by longitudinal modes. It is difficult to imagine very much ultrasound straying to a neighboring position and scattering back to the receiver. An exception is a position next to a break. Reflections off the break surface may show up in the received signal.

Figure 14 shows waveforms collected from two positions on Udimet 520 specimen B2. The dashed line waveform is from the position at 0.5 inches, which is next to the break location. The solid line waveform is from the position at 2.0 inches, which is far from the break and actually in the 50 per cent life region. Both waveforms are reminiscent of a ring down rather than an ultrasonic decay signal. On examination one can see the position next to the break rings at a higher frequency than the position far from the break.

Figure 15 shows the frequency magnitude spectra of the time signals in figure 14. They bear the same information as in figure 14. The signal has a narrow frequency range, typical of a ring down, and the position next to the break has the higher frequency. In order to cover the frequency range appropriate for all these waveforms the analysis will be for 1.9 to 2.9 MHz.

Figure 16 shows the UD rates on specimen B2 as a function of position. In figure 16a the regressions were carried out over the full 10 microseconds of the waveforms. This profile

does not identify the location of the break but it does seem to differentiate between the 100, 50, and 25 percent used up life sections.

On the other hand the regressions over the first 2 microseconds, shown in figure 16b, do identify the break location but do not differentiate the different used up life sections. This indicates that the first 2 microseconds of the signal sees the break much better than does the rest of the signal. But does not have information on the general condition of the material environment it is in.

Figures 17a and 17b show the mean times, $\langle t \rangle$, for specimen B2. The same comments about detectability of the break and of degree of used up life can be made here as were made with UD rate. The $\langle t \rangle$ plots are very much the mirror image of the UD rate plots in figure 16.

Figure 18 shows the profile of the centroid of the power spectrum for specimen B2. The centroid of the total waveform in figure 18a exhibits sensitivity to both the break location and also to degree of used up life, even out to the 12.5 per cent region. Besides this, it has far less scatter than any of the other plots. Calculation of centroid for 7 to 9 μ seconds is shown in figure 18b. As with the UD rate and the mean time, the centroid in the first 2 μ seconds is the most sensitive to the presence of the break. It is also sensitive to the degree of used up life. The 7 to 9 μ seconds has more scatter because it is calculated from fewer waveform data points.

The centroid in this experiment increases with degradation of the material. In the two earlier cases we saw that the centroid decreased with disorder. In case 1 the disorder was matrix porosity. In case 2 it was matrix cracking. These were attributed to increase in ultrasonic attenuation. It is likely that in the present case the centroid change is not related to attenuation. We noted above that signals from positions next to a break may be special because they contain reflections off the break surface. This may effect the difference we see in the centroid.

Case 4: Detecting Surface Layer Formation in T-650-35/PMR-15 Polymer Matrix Composites Panels due to Thermal Aging.

It was established by destructive means that thermal aging in air causes the formation and growth of undesired surface layers on this material. There is a temperature threshold for this phenomenon between 500 and 550 F.

It was the object of this work to examine whether A-U can detect the formation of this layer.

A total of 12 four inch by four inch woven fiber panels were studied in three thicknesses. They were 0.13 cm (4 ply), 0.25 cm (8 ply), and 0.75 cm (20 ply). A panel of each thickness were thermally aged at 400, 500, 550, and 600 F.

Figure 19 shows an A-U waveform collected on 0.13 cm specimen PD2 prior to any thermal aging. The data were collected using 0.5 MHz broadband transducers. The early,

post dead time, portion of this waveform exhibits pulses due to the lowest symmetric and the lowest antisymmetric Lamb modes. The lowest symmetric pulse arrives at about 15 microseconds into the time record and the lowest antisymmetric arrives at about 35 to 45 microseconds. As mentioned earlier, the symmetric pulse arrives earlier and has displacement primarily in the propagation direction. The antisymmetric pulse arrives later and is shear like, with displacement normal to the surface. The antisymmetric pulse therefore is seen as larger by the receiving transducer, which is more sensitive to normal displacements. These Lamb wave pulses dominate the initial rise in the A-U waveform. (There is also an antisymmetric pulse at 80 to 90 microseconds which is a reflection from one of the panel edges.)

The symmetric Lamb wave travels at the longitudinal velocity in the plate⁴. We can then use its arrival time to make a rough calculation of the longitudinal velocity in these specimens. Since the transducers are separated by 3.4 cm and the pulse arrives at about 15 microseconds we can say the longitudinal velocity, V , is ~ 0.23 cm/ μ sec, which is reasonable for a polymer material. In order to compare specimens of three thicknesses under similar Lamb wave conditions we calculate the through thickness resonance condition for each:

$$h = \lambda/2 = V/2f$$

The resonance frequency is:

$$f_{\text{res.}} = V/2h$$

For a given panel thickness, h , we expect plate wave behavior at frequencies below $f_{\text{res.}}$ and ultrasonic decay behavior at frequencies above.

If we apply this to panels of all thicknesses h :

Table 1

For the thin panels	$h = 0.13$ cm,	$f_{\text{res.}} = 0.88$ MHz.	$f_{\text{filt}} = 0.3 - 0.6$ MHz
For the medium panels	$h = 0.25$ cm,	$f_{\text{res.}} = 0.46$ MHz.	$f_{\text{filt}} = 0.155 - 0.31$ MHz
For thick panels	$h = 0.75$ cm,	$f_{\text{res.}} = 0.15$ MHz.	$f_{\text{filt}} = 0.075 - 0.15$ MHz

In general, we will always calculate ultrasonic decay rates for filters, f_{filt} , entirely above $f_{\text{res.}}$. In table 1 the last column shows, instead, appropriate frequency ranges for plate wave behavior for each thickness. In this experiment we found it to be useful to treat the plate wave time segment, which is before and up to the peak in the signal, as a “reverse” ultrasonic decay and to calculate a rise time using the UD rate algorithm.

Figures 20a and 20b show the log of zero moment, $\text{Log}(M_0)$, plots for two different frequency filters on the thin specimen of figure 19. Figure 20a was obtained with the plate wave filter of 0.3 to 0.6 MHz. Here the plate wave rise phenomenon is clearly evident between 10 and 40 microseconds. In 20b, the filter is 0.5 to 0.9 MHz. This is

above the plate wave region and is a fairly smooth log plot starting at 10 microseconds and passing beyond the 40 microsecond end of the plate wave region. Figure 20 shows that very different information is obtained from different portions of the frequency spectrum of the same waveform.

For the thick specimen, PD5, the waveform in figure 21 does not display the pronounced Lamb Wave pulses seen for the thin specimen in figure 19.

Figure 22a displays log M0 with the filter 0.075 to 0.150 MHz, the plate wave region as dictated by table 1. This shows the early plate wave rise portion even though the original waveform in figure 21 masks it.

Figure 22b displays log M0 with the filter 0.5 to 0.9 MHz for specimen PC5. As with the thin panel the higher frequency filter shows UD decay regression. All the panels, including the medium thickness set, were analyzed the same as these at every aging stage where A-U data was collected.

Rise time results

As mentioned earlier, a typical A-U signal, $\phi(t)$, has an initial dead time, then a rise segment followed by an exponential decay segment. We calculate the rise times here in that rise segment. The actual time range used is 10 to 40 microseconds to include the lowest symmetric and lowest antisymmetric plate pulses.

Figures 23 a, b, and c show the results of analyzing this Lamb wave portion of the waveforms. A rise rate, ($= -\beta$), is plotted against thermal aging time. The rise times here, as well as the standard deviations, are from averaging the set of 16 on each specimen. For each thickness of specimens aged at 550 and 600 F, (above the layer formation threshold), there is an initial decrease in rise time compared to the 400 and 500 F specimens. This decrease in rise time is taken as due to the thermally formed layer acting as a barrier to the emergence of the antisymmetric Lamb wave pulses at the surface. Eventually, after about 1000 hour at temperature, the layer itself appears to become thick enough to support Lamb waves and the rise time increases again. The thick specimen heated at 550 F behaves similar to the 4 ply and 8 ply heated to 550 F but seems to go through the thermal layer transformations more rapidly. The thick specimen heated to 600 F does not behave as the others. It is possible that the results were altered by delaminations in this case.

Case 5: Detecting Spin Test Degradation in PMC Flywheels.

These are being considered as alternates, or complements, to chemical batteries for several NASA aerospace energy storage applications. Fourteen flywheels covering five different sets of fabrication parameters, designated as a, b, c, d, and e, were to be tested nondestructively before and after subjecting them to spin stresses typical of high load applications.¹⁹

The experimental flywheels were 17.5 cm diameter aluminum hub with a 5.7 cm PMC annular ring bonded to them. It was integrity of the PMC ring that was to be studied.

Several transducer orientations were tested, but the most useful turned out to be measurement with 0.1 – 0.2 MHz transducers, coupled through RTV pads, about 3.0 cm separated along the 5.0 cm wide edge of the rings. The ultrasound traveled along the radius towards the hub. From the sender, to the hub, and then back to the receiver was about 11 to 12 cm. It was noted in the previous case that a cross ply longitudinal velocity in a PMC might be taken as $V \sim 0.23 \text{ cm}/\mu\text{sec}$. This would imply, in this case, a round trip time of about 50 μsec . Figure 24 shows example waveforms collected in this transducer orientation on the same specimen both before and after the spin test. There is a prominent pulse at about 50 μsec . Since measurement across the diameter showed no detectable signal it was judged that the signal received after 50/ μsec was due to multiple reflection within the PMC ring and not the hub. The primary difference between the two waveforms is that the after spin waveform of figure 24b is much diminished in magnitude from the before spin waveform of figure 24a.

Due to the high attenuation of this material in this orientation the 0.1 – 0.2 MHz transducers produced power spectra that peaked between 0.05 and 0.15 MHz. Ultrasonic Decay rates were calculated using this frequency filter. The log power spectrum plots were fairly linear for the time partition 50 to 300/ μsec . Figure 25 shows the UD rate results for the 14 flywheels separated according to the 5 sets of fabrication parameters, a, b, c, d, and e. The data plots are averages for the 24 measurements on each ring. There were 3 measurements at each of 8 locations equally spaced around the rings. These results reflect the fact that the fabrication conditions d and e produced more uniform rings than did the others. The UD rates for conditions d and e are lower after the spin tests than before showing the change that occurred.

DISCUSSION AND CONCLUSIONS

Three analysis parameters were studied in this work:

Ultrasonic Decay rates, Signal time domain mean times, and Centroid of the power spectrum. Additionally, a unique application of Lamb wave analysis is demonstrated.

An important consideration in designing experiments is choice of frequency range to employ. This dictates the types of ultrasonic wave modes one can expect. Generally speaking, if one wishes to analyze Lamb waves it is required to work at relatively low frequencies, certainly below the through thickness resonance frequency. Lamb wave analysis has the advantage over the other three parameters in that one obtains the absolute physical variables of wave velocity and hence stiffness moduli. A draw back to Lamb wave analysis for mechanical modulus is that it puts restrictions on the geometries one can apply it to. One must be able to use frequencies that see the specimen as a plate. One must be able to identify the first arrival of the lowest symmetric and antisymmetric plate modes. In addition, it is desirable that the thickness must be constant. One also requires a range of transducer separations, which places a minimum on the amount of surface area needed. Lamb wave velocities cannot be determined at a single point.

The other three analysis tools; Ultrasonic Decay rates, Signal mean time, and Centroid of the power spectrum do not provide absolute physical variable results. This makes them “before and after” comparison tools. We saw cases where each of these tools were capable of detecting differences in material/mechanical properties in specimens. This was so in comparing specimens of the same architecture but different texture, specimens before and after thermomechanical treatment, and also differences in condition for different positions on the same specimen.

An approach to applying A-U to a new situation can be to look for changes in the calculated parameters that coincide with the changes that are happening in the material/mechanical specimens under study. In some situations, such comparing of specimens with different textures such as density, or else for before and after tensile loading, it is possible to predict the effect on one or more of the calculated parameters. In other cases, such as with alloys having different states of creep life, or in PMCs with different stages of thermal aging, the results may not be initially predictable.

The UD rate

Application of ultrasonic decay to analysis of A-U signals requires identifying an exponential decaying region of the signal. An aid in this may be the practice of DC zeroing of the waveforms to be analyzed.

By now the “oldest” of the new analysis techniques, UD rate, has been well established on CMCs. As the first two example cases, and several of the references, especially in the HITemp program, testify, UD rate has really been very successful with CMCs. With CMCs it is easy to understand the mechanisms that relate UD rate to the properties of the CMCs such as porosity and crack densities.

This is less evident with MMCs. The ability to detect, for example, tensile fatigue,¹⁴ has been shown. But the relationship to changes in material/mechanical properties is less as clear as with the CMCs.

It is something of an irony that for PMCs, the materials on which A-U was first established, the UD rate had always been unsuccessful. This has been true until the work shown in case 4. Here the application of UD analysis to lowest mode plate waves was successful in monitoring the effect of thermal treatment on material properties. Case 5 results the UD rate also shows promise with PMC Fly Wheels.¹⁹

Case 3 shows that UD rate can be applied to non-composite materials. Besides this creep fatigue study, UD rate has also shown promise in other alloy structures such as engine rotors, etc. This appears to be an important future use. It will be desirable to develop models for how the UD rate interacts with non-composite material/mechanical properties.

The meantime

The meantime of the A-U signal, $\langle t \rangle$, can give the same information as the UD rate. An advantage of $\langle t \rangle$ is that it does not seem to require determination of a pure exponentially decaying region of the signal. An advantage of the UD rate is that it is more directly

related to ultrasonic attenuation. UD rate, β , increases with ultrasonic attenuation, mean time $\langle t \rangle$ decreases with attenuation. As an alternate to $\langle t \rangle$ we defined a skewing factor, s , which varies between 1 and -1 and increases with increasing attenuation.

In principal, this parameter gives the same information as the UD rate. If you have a waveform that is a perfect exponential decay then there will be a β , and there will be a $\langle t \rangle$. You could calculate one from the other. But when the waveform is not a perfect exponential decay then the mean time frees you of identifying a region of perfect exponential. In some situations you might not have that. And so the mean time is your only alternative. However, the UD rate, being more closely related to ultrasonic attenuation, has the better hope of being related to material/mechanical properties.

The Centroid of the Power Spectrum

The Centroid of the power spectrum is a measure the shape of the frequency magnitude spectrum. Changes in this may be related changes in attenuation or other characteristics of the collected A-U signal.

It is unclear why the centroid behaves as it does. If a specimen is manipulated thermomechanically to produce some type of degradation we can usually expect the UD rate to go up and the mean time to go down. However we have found that the centroid goes up in some cases and goes down in others. We expect that a degradation step might produce ultrasonic attenuation, and this will affect higher frequencies more than lower. So this ought to lower the centroid. When the centroid increases something else must be happening. It would be desirable to develop models to explain the relationship between the changes in centroid and material/mechanical properties.

If degradation decreases signal strength the change in signal to noise may change the centroid. This would mean the centroid is dependent on signal magnitude. Rather than use the centroid under this circumstance it would be more direct to use one of the moments of the frequency spectrum.^{9,18}

DC Zeroing of Waveforms

It was shown that the practice of initially subtracting the DC component of waveforms sometimes gave better results. The primary advantage was in extending linear range for Log Power Spectrum regressions for Ultrasonic Decay rate calculations.

Finally, it should be noted that with proper choice of initial conditions for collecting acousto-ultrasonic waveforms all the discussed parameters can be determined from the same data and provide a wealth of information on the condition of the specimens under study.

APPENDIX A

A Brief Description of Lamb Wave Analysis of A-U Signals.

H. Lamb worked out the permitted propagation modes for ultrasonic waves in a plate.²⁰ In figure A1 the phase velocities of these modes are plotted against (frequency)×(plate thickness). Note that only the lowest symmetric, L_{11} , and lowest antisymmetric, L_{21} , have significant frequency ranges for which the phase velocity is independent of frequency. They are non-dispersive in these ranges and can be observed as pulses in a broadband signal. The group velocities of these two modes is much greater than that of the higher, very disperse, modes. Thus they arrive earlier. Figure A2 shows the result of windowing the early part of a signal composed of all these modes.²¹

Tank and Henneke⁴ devised an approximate theory for the Lamb wave analysis that allowed extraction of mechanical modulus information from these two lowest modes. Their experiment employed narrow band tone burst signals. The time of arrival of a chosen peak, t , was plotted against the separation, s , of transducers coupled in the A-U configuration. For several s , t , combinations a velocity:

$$\text{Velocity} = \delta s / \delta t$$

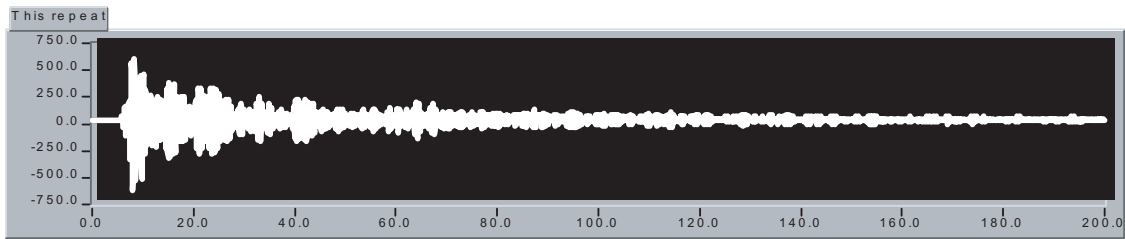
Could be determined, and hence a mechanical modulus.

Later, Kautz⁵ developed a technique for applying the Tang Henneke experiment to broadband signals. An advantage of this is that, with filtering, velocities could be determined over a range of frequencies in the broadband signal. Figure 19 in the present work shows a waveform of this type collected on a 4 ply, T-650-35/PMR-15 PMC panel. The lowest symmetric pulse arrives at about 15 microseconds into the time record and the lowest antisymmetric arrives at about 35 to 45 microseconds.

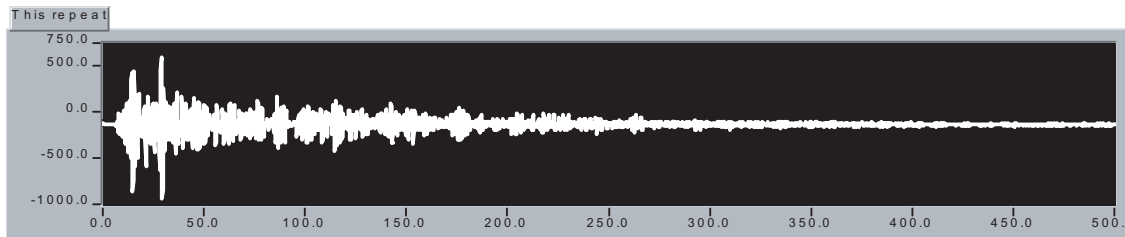
REFERENCES

1. A. Vary and K.J. Bowles, "Ultrasonic Evaluation of the Strength of Unidirectional Graphite Polyimide Composites," Proceedings of the Eleventh Symposium on Nondestructive Evaluation, ASNT, San Antonio, TX, (1977) pp. 242–258. NASA TM X-73646.
2. A. Vary and K.J. Bowles, "Use of an Ultrasonic-Acoustic Technique for Nondestructive Evaluation of Fiber Composite Strength," Reinforced Plastics—Contact 78, Proceedings of the 33rd Annual Conference, Society of the Plastics Industry, New York, 1978, Section 24–A, pp. 1–5.
3. A. Vary and R.F. Lark, "Correlation of Fiber Composite Tensile Strength with the Ultrasonic Stress Wave Factor," J. Test. Eval., Vol. 7, No. 4, July 1979, pp. 185–191.
4. Tang, B. and Henneke II, E.G., "Long Wavelength Approximation for Lamb Wave Characterization of Composite Laminates," Res. Nondestr. Eval., Vol. 1, No. 1, 1989, pp. 51–64.
5. Kautz, H.E., "Detecting Lamb Waves with Broadband Acousto-Ultrasonic Signals in Composite Structures," Res. Nondestr. Eval., Vol. 4, 1992, pp. 151–164.
6. Weaver R.L., "Diffuse Field Decay Rates for Material Characterization," Solid Mechanics Research for Quantitative Nondestructive Evaluation, Eds. J.D. Achenbach and Y. Rajapaskie, Martinus Nijhoff Publishers, Netherlands, 1987, pp. 425–434.
7. Lott, L.A., Kunerth, D.C., and Characklis, G.W. "Acousto-Ultrasonic NDE of Ceramic Matrix Composites," Presented at the International Gas Turbine and Aeroengine Congress and Exposition. Orlando, FL, June 3–6 1991.
8. "Signal Analysis," A. Papoulis, McGraw-Hill, 1977
9. Tiwari, A., Henneke, II, E.G., and Duke, J.C., "Acousto-ultrasonic (AU) Technique for Assuring Adhesive Bond Quality," J. Adhesion, 1991, Vol. 34, pp. 1–15
10. Kiernan, M.T., Duke, Jr., J.C., "Acousto-Ultrasonics as a Monitor of Material Anisotropy," Mater. Eval. Vol. 46, pp. 1105–1113. (1988).
11. Kautz, H.E., "Effects of Transducer Coupling and Specimen Support Structure on Reproducibility in Ultrasonic Decay Measurements," HITEMP Review 1999, NASA/CP—1999-208915/Vol2, (1999), Paper 51.

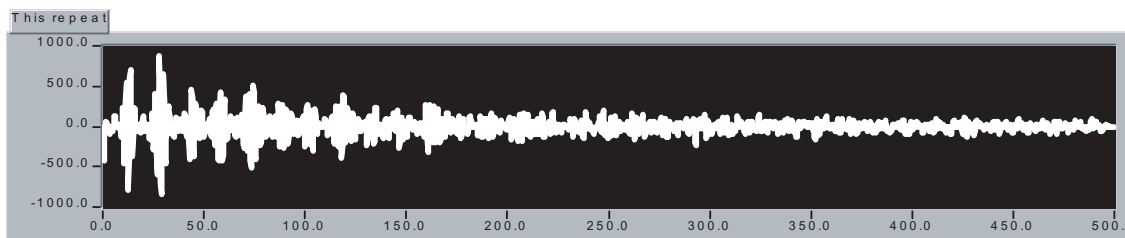
12. Kautz, H.E., "New Acousto-Ultrasonic Techniques Applied to Aerospace Materials," Conference on Non-Destructive Testing and Evaluation for Manufacturing and Construction," University of Illinois, Urbana, IL, (1988), NASA TM-101299.
13. Roth, D.J., Kautz, H.E., Abel, P.B., Whalen, M.F., Hendricks, J.L., and Bodis, J.R., "Three Dimensional Surface Depression Profiling Using Focused Air Coupled Ultrasonic Pulses," *Mat. Eval.*, Vol. 59, p. 543, April 2001.
14. Kautz, H.E., Bowman, C., and Baaklini, G.Y., "Comparison of Contact and Non-Contact Acousto-Ultrasonic NDE on Fatigue Cycled SCS-6/Ti 6-4 Metal Matrix Composite Tensile Specimens," To be published (2001).
15. *Nondestructive Testing Handbook*, Vol. 7, Ultrasonic Testing, Second Ed., ASNT, 1991, p. 841.
16. Kautz, H.E., "Acousto-Ultrasonic Decay in Metal Matrix Composite Panels," NASA TM-106972, August 1995.
17. Kautz, H.E. and Bhatt, R.T., "Ultrasonic Velocity Technique for Monitoring Property Changes in Fiber-Reinforced Ceramic Matrix Composites," 15th Annual Conference on Composites and Advanced Ceramics sponsored by the American Ceramic Society, Cocoa Beach, Florida, January 13-16, 1991. NASA TM-103806.
18. Gyekenyesi, A.L., Kautz H.E., and Cao, W., "Damage Assessment of Creep Tested and Thermally Aged Udimet 520 Using Acousto-Ultrasonics," NASA/TM-2001-210988, (2001).
19. Baaklini, G.Y., Kautz, H.E., Gyekenyesi, A.L., Abdul-Aziz, A., and Martin, R.E., "NDE for Material Characterization in Aeronautic and Space Applications," NASA/TM-2000-210474, December 2000.
20. H. Lamb, *Proc. R. Soc. London. A* 93:114 (1917).
21. Roth, Don J., Harmon, Laura M., Martin, Richard E., Gyekenyesi, Andrew L., and Kautz, Harold E., "Development Of A High-Performance Acousto-Ultrasonic Scan System," Twenty-ninth Annual Review of Progress in QNDE, Western Washington Univ., Bellingham, Washington, July 14-19, 2002.



(a)

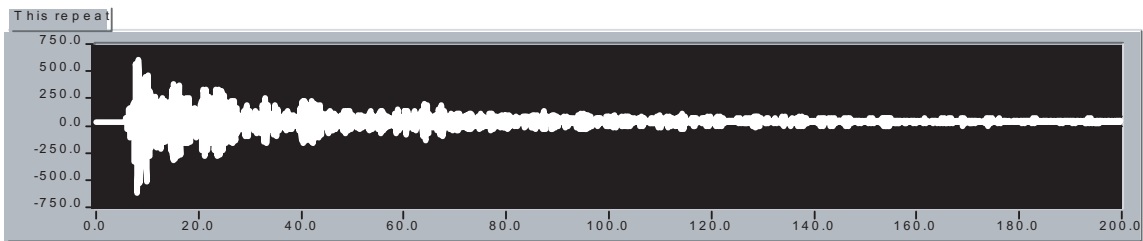


(b)

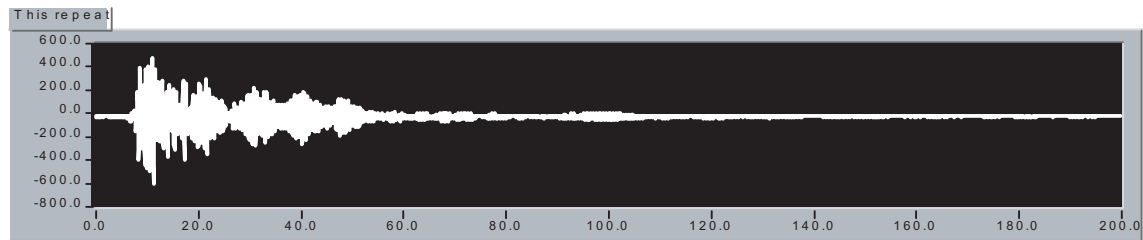


(c)

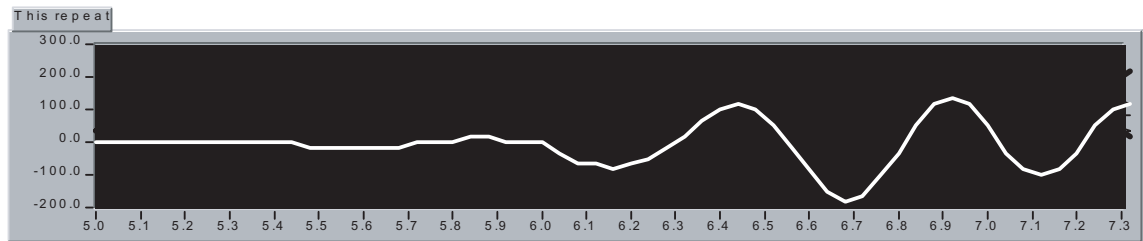
Figure 1.—Waveforms in different frequency ranges for SiC/RBSN fully dense specimen - 19. (a) Waveform with 2.25 MHz transducers, $V/fh = 1.62$. (b) Waveform with 1.0 MHz transducers, $V/fh = 3.65$ (c) Waveform with 0.5 MHz transducers, $V/fh = 7.3$



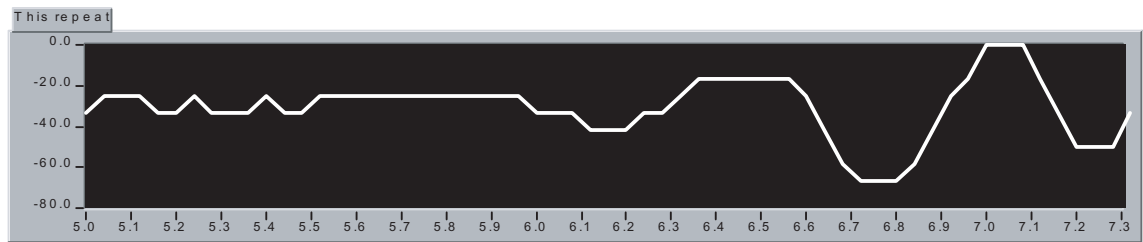
(a)



(b)



(c)



(d)

Figure 2.—Collected waveforms on two SiC/RBSN CMCs. (a) Fully dense matrix specimen 19. (b) 30 percent porous matrix specimen 99. (c) Specimen 19, 5.0 to 7.3 μ sec. Portion of A-U Signal. (d) Specimen 99, 5.0 to 7.3 μ sec. Portion of A-U Signal.

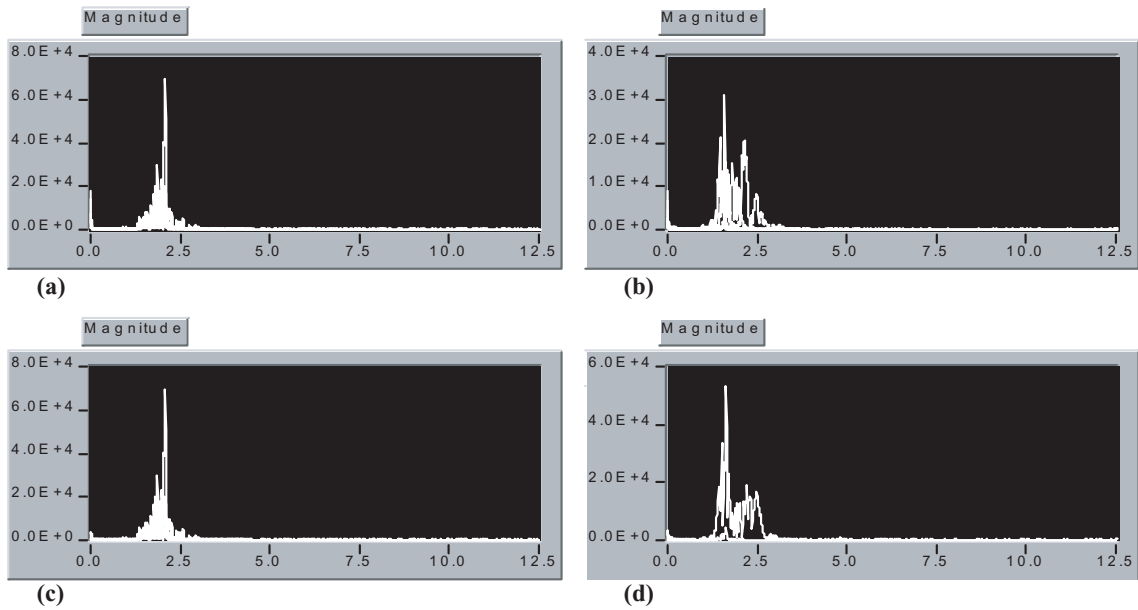
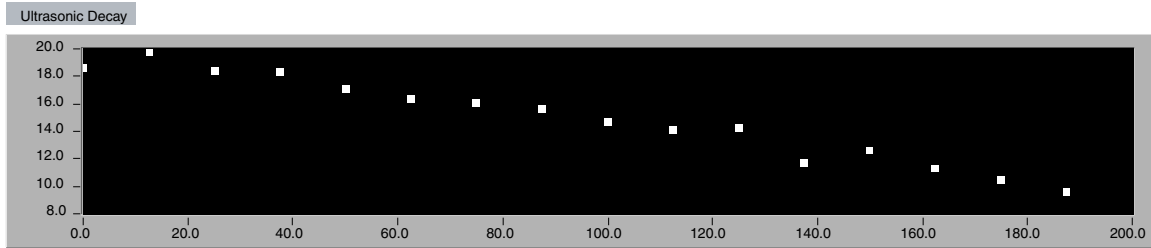
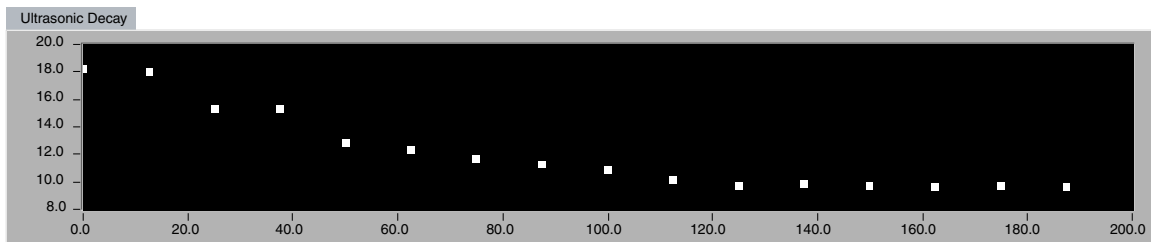


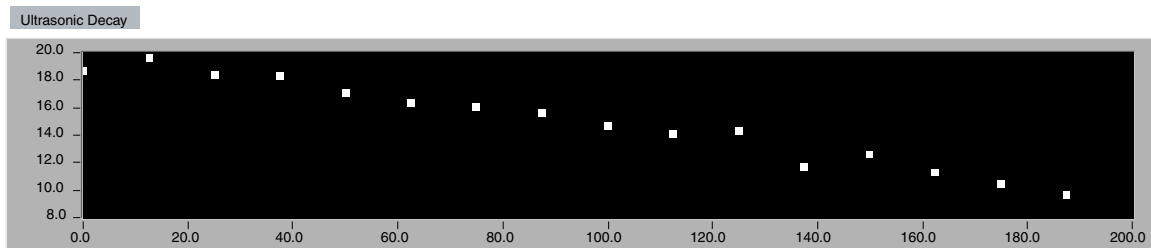
Figure 3.—Magnitude spectra on two SiC/RBSNCMCs. (a) Specimen 19 with no DC zeroing. (b) Specimen 99 with no DC zeroing. (c) Specimen 19 with DC zeroing. (d) Specimen 99 with DC zeroing.



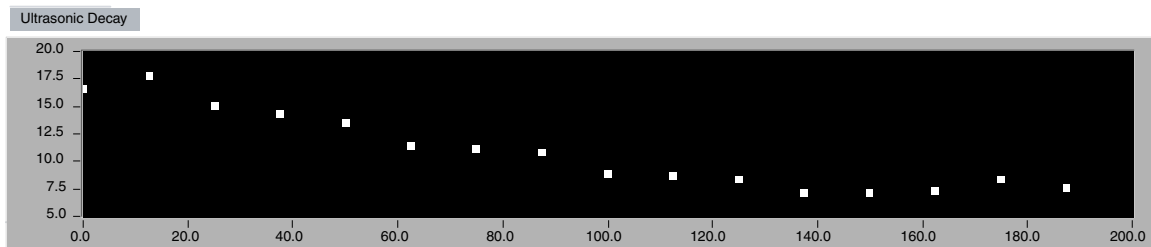
(a)



(b)



(c)



(d)

Figure 4.—Log of power spectrum integrals—without waveform DC zeroing (a) fully dense specimen 19 and (b) 30% porous specimen 99. Log of power spectrum integrals—with waveform DC zeroing, (a) fully dense specimen 19 and (b) 30% porous specimen 99.

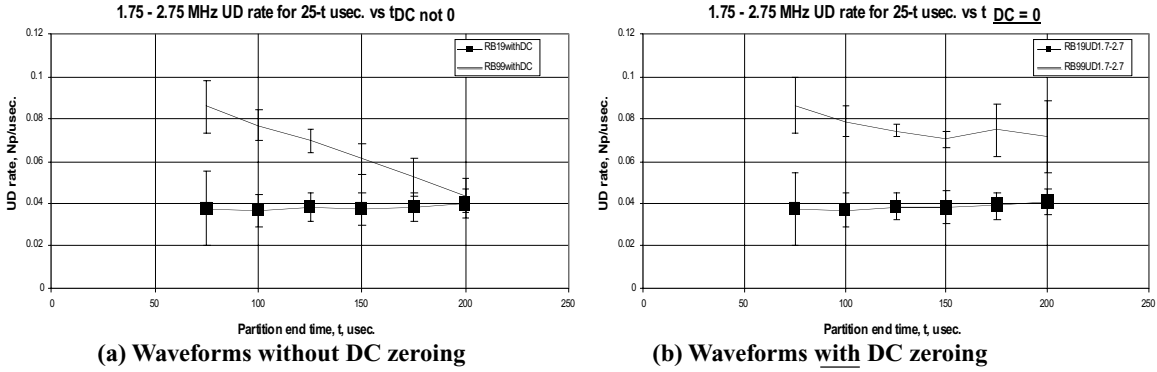


Figure 5.—1.75 to 2.75 MHz UD rates comparing data from waveforms not DC zeroed to waveforms with DC zeroed.

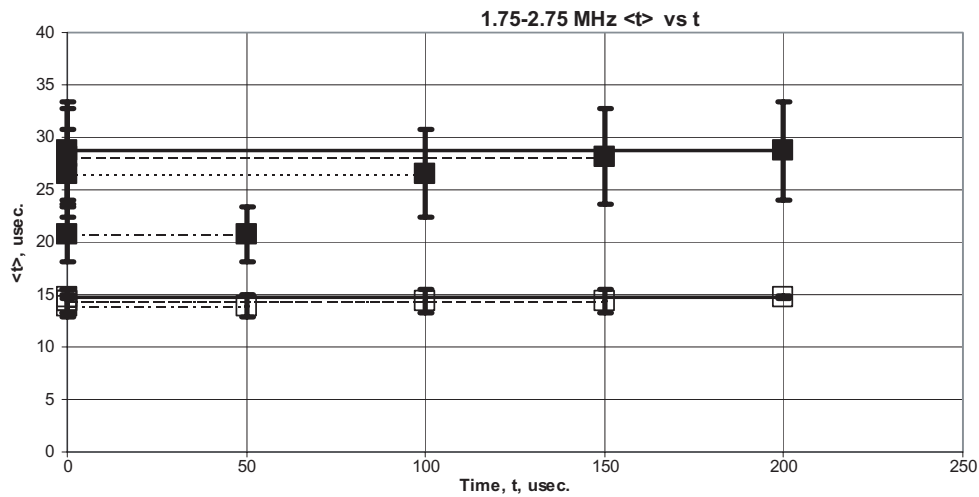


Figure 6.—1.75 to 2.75 MHz mean time vs time span for calculation for the two [0] SiC/RBSN CMCs

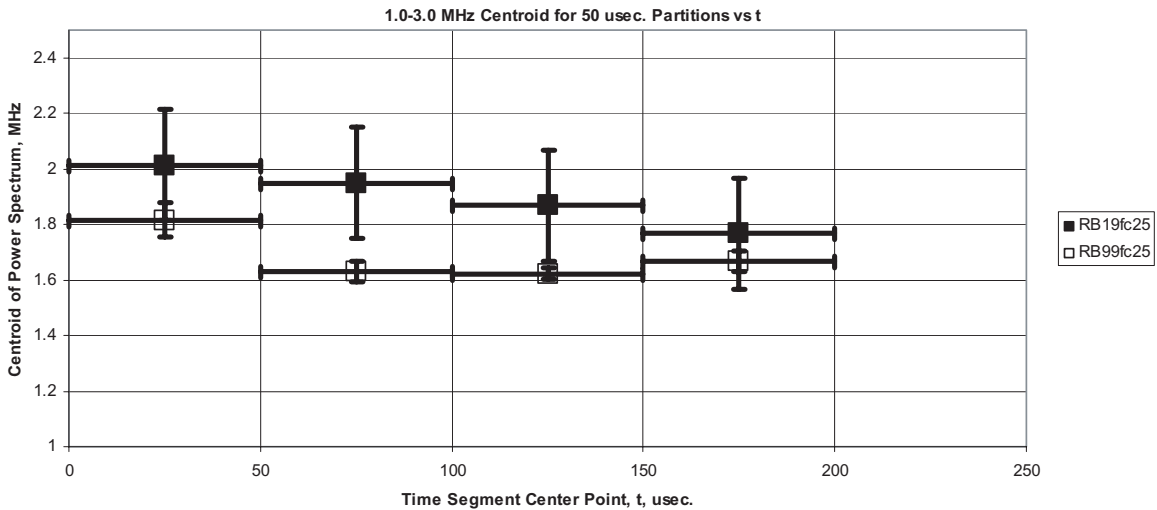
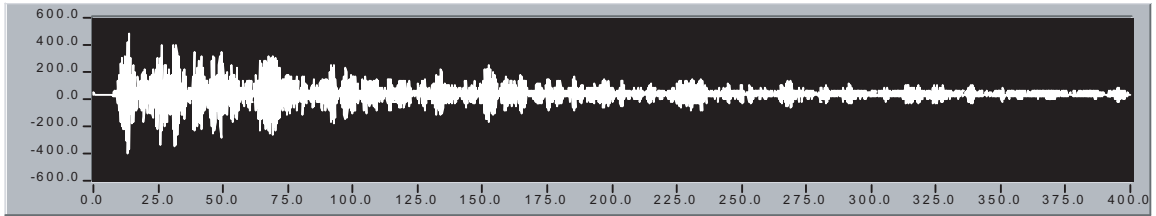
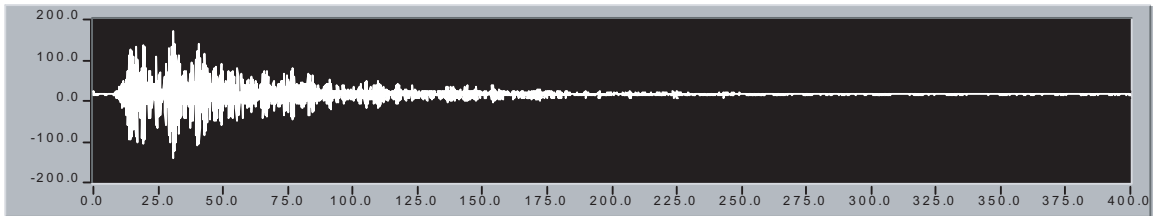


Figure 7.—1.0 to 3.0 MHz Centroid for 50 microsecond partitions vs center time of partition.

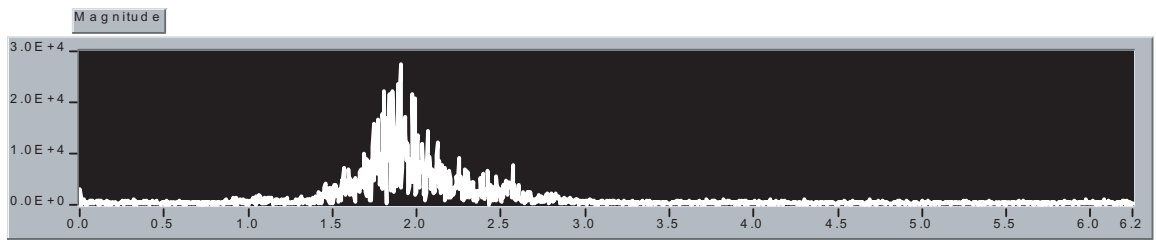


(a)

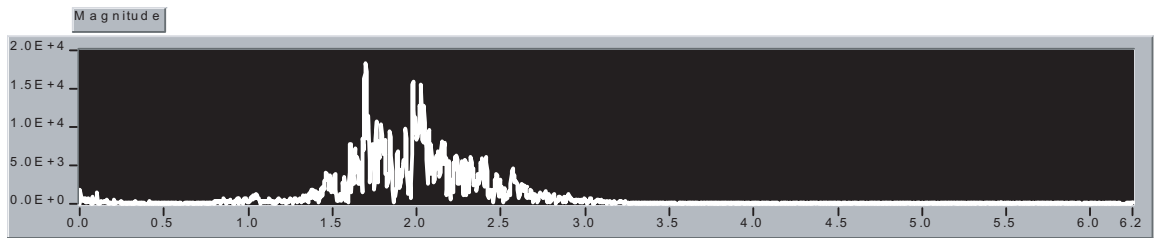


(b)

Figure 8.—A-U waveforms collected on ± 45 SiC/SiC CMC's. (a) Specimen 32 not tensile cycled. (b) Specimen 28 tensile tested with 10,000 cycles to 10 ksi.

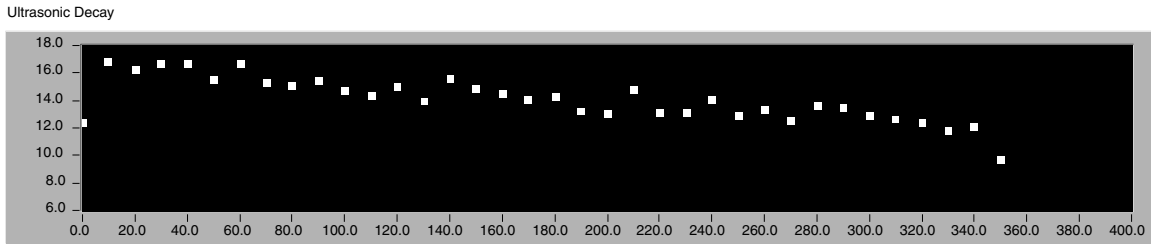


(a)

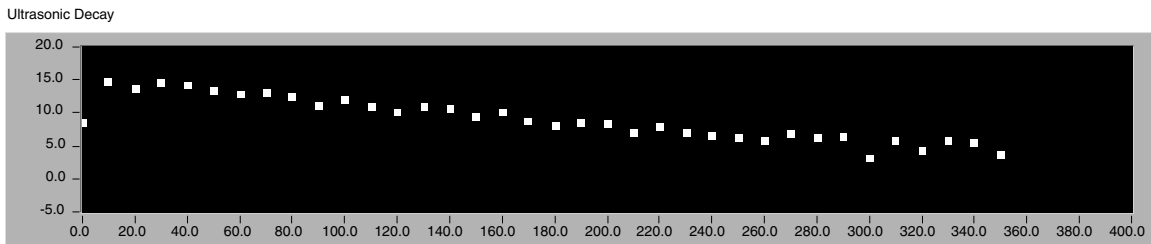


(b)

Figure 9.—Frequency magnitude spectra for ± 45 SiC/SiC CMCs. (a) Specimen 32 not tensile cycled. (b) Specimen 28 tensile tested for 10,000 cycles to 10 ksi.



(a)



(b)

Figure 10.—Log of power spectrum integral vs time. (a) Specimen 32 not tensile cycled. (b) Specimen 28 tensile tested for 10,000 cycles to 10 ksi.

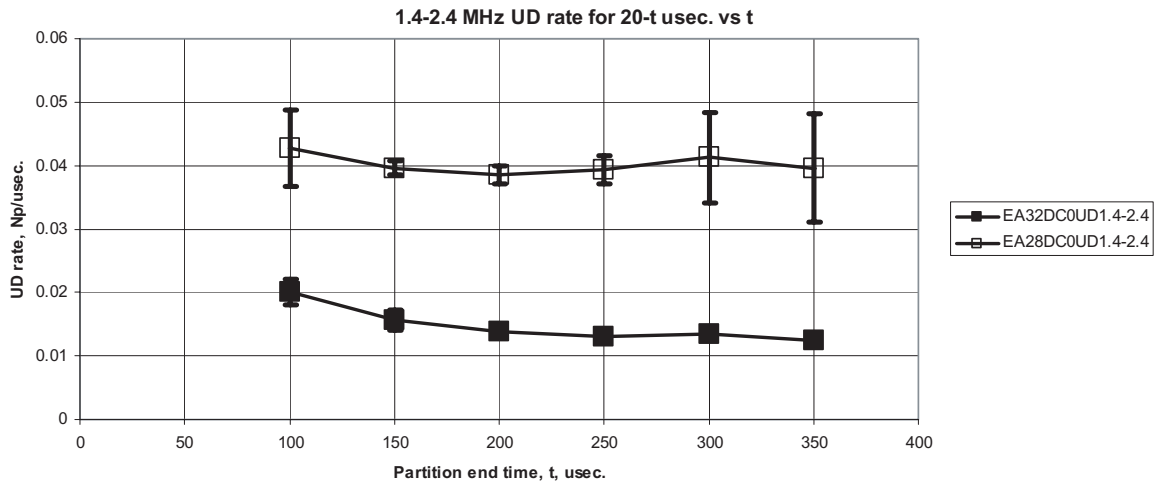


Figure 11.—1.4 to 2.4 MHz UD rate for 20-t μ sec. Vs t.

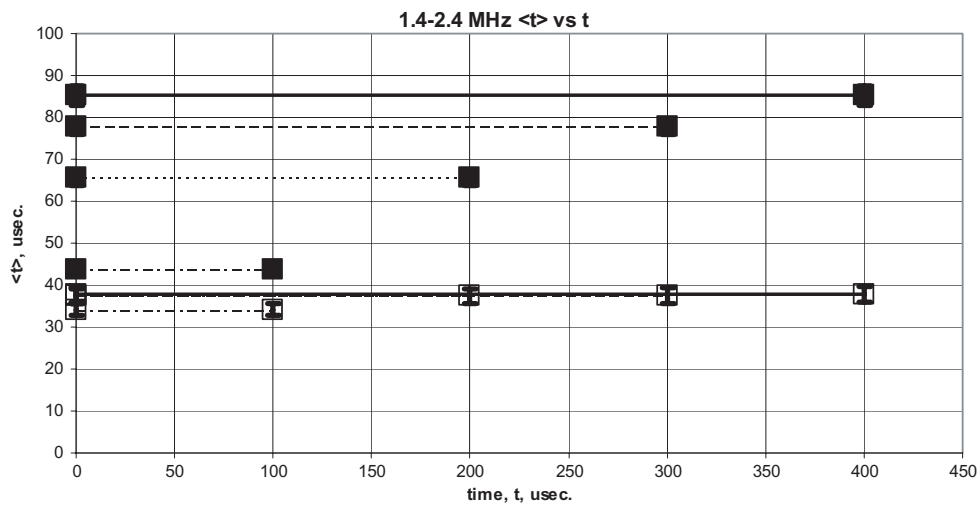


Figure 12.—Mean time, $\langle t \rangle$, for SiC/SiC ± 45 specimens.

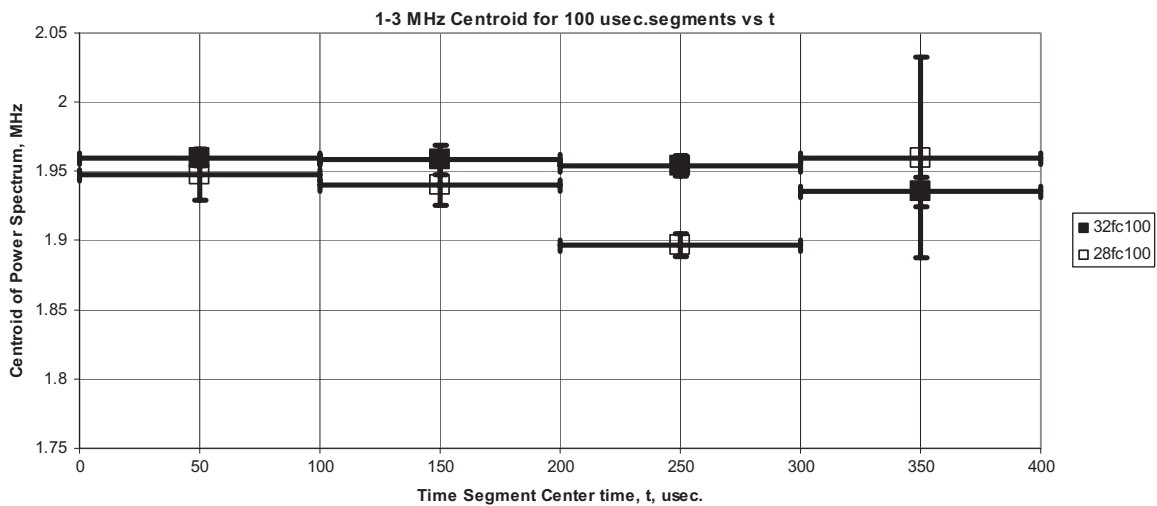


Figure 13.—Centroid of the power spectrum for SiC/SiC ± 45 specimens.

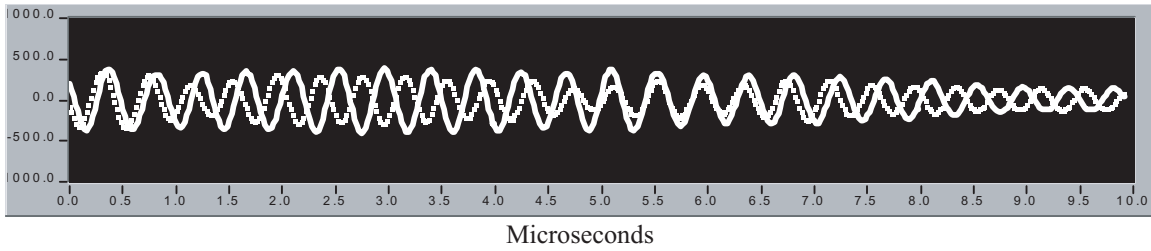


Figure 14.—Two waveforms from UDIMET 520, specimen B2.

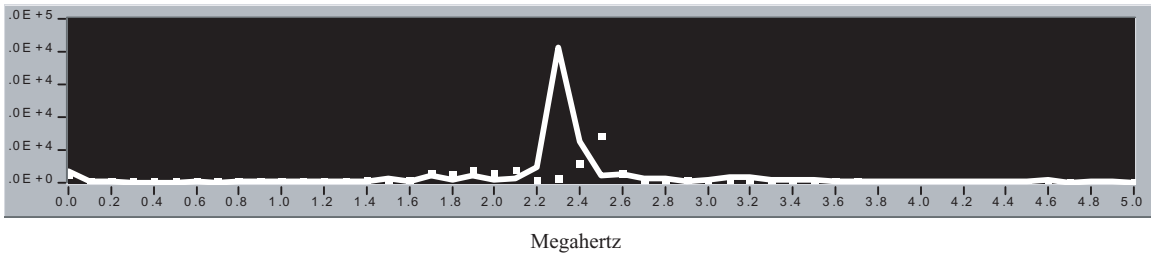


Figure 15.—Frequency spectra from the two UDIMET 520 waveforms of Figure 14.

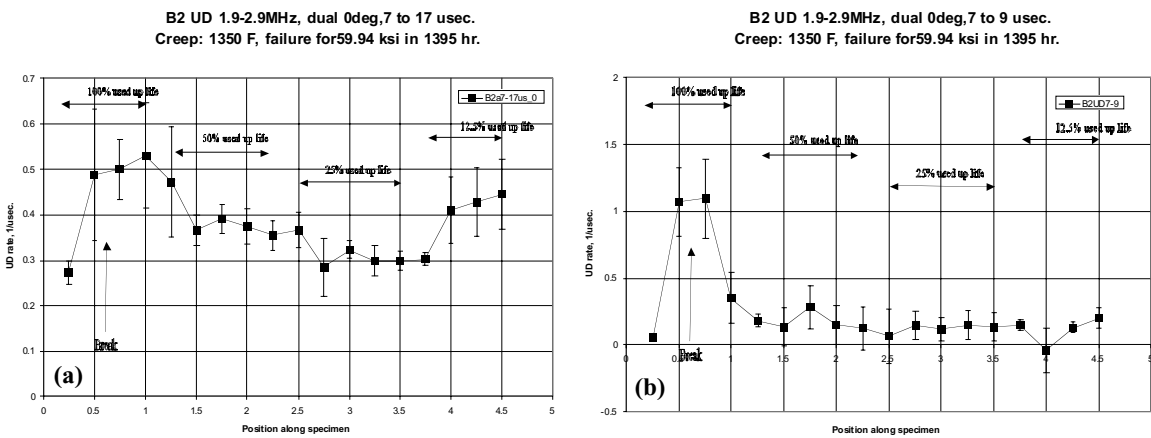


Figure 16.—UD rate on UDIMET 520 specimen B2. (a) 7 to 17 microseconds. (b) 7 to 9 microseconds.

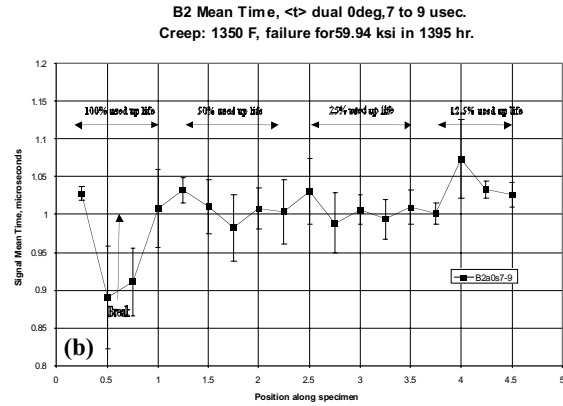
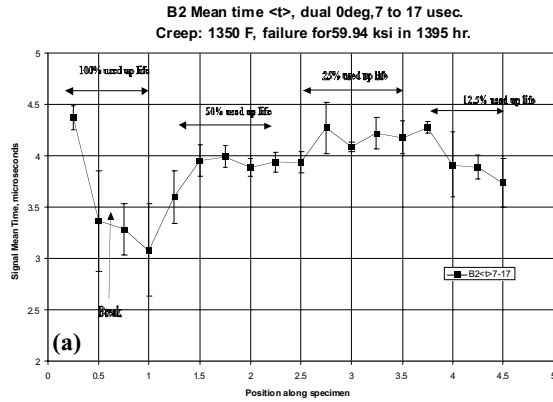


Figure 17.—Mean time $\langle t \rangle$, on UDIMET 520 specimen B2. (a) 7 to 17 microseconds. (b) 7 to 9 microseconds.

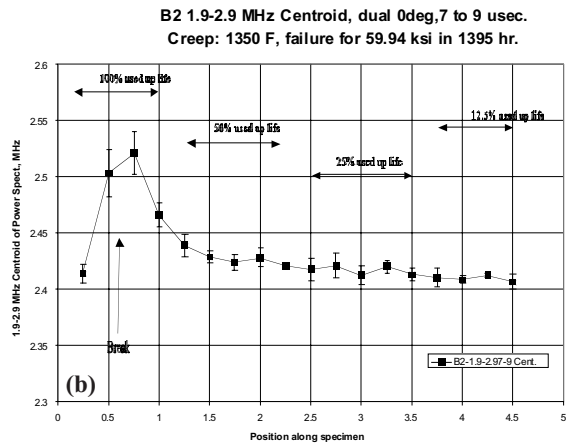
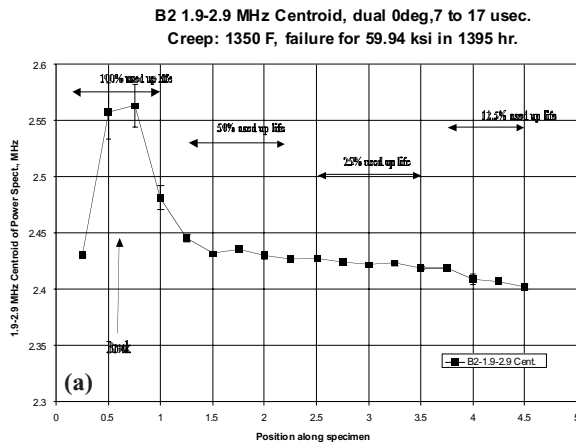


Figure 18.—Centroid on UDIMET 520 Specimen B2. (a) 7 to 17 microseconds. (b) 7 to 9 microseconds.

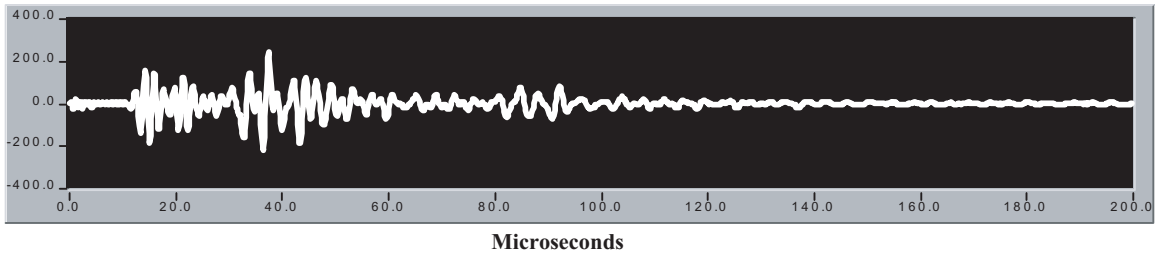
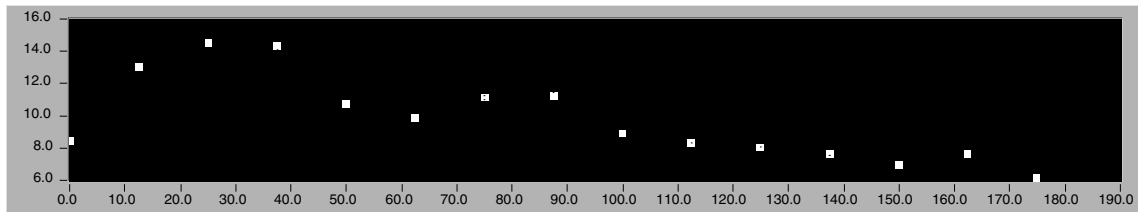
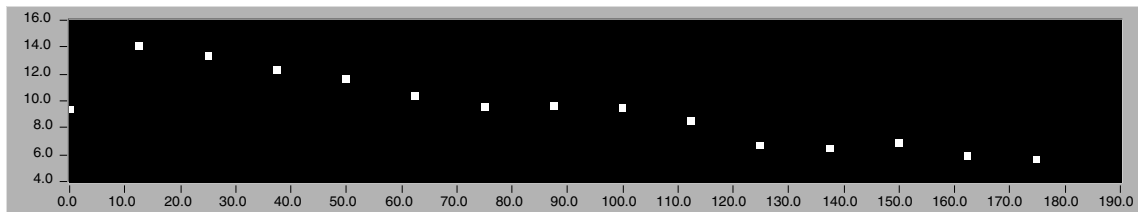


Figure 19.—Acousto-ultrasonic signal for unaged 4-Ply, 0.13cm thin T-650-35/PMR-15 specimen PD2.



(a)



(b)

Figure 20.—Ultrasonic decay for un-aged 4-ply, 0.13 cm thin T-650-35/PMR-15 specimen PD2. (a) Ultrasonic decay graph with 0.3 to 0.6 MHz filtered zero moment of the power spectrum. (b) Ultrasonic decay graph with 0.5 to 0.9 MHz filtered zero moment of the power spectrum.

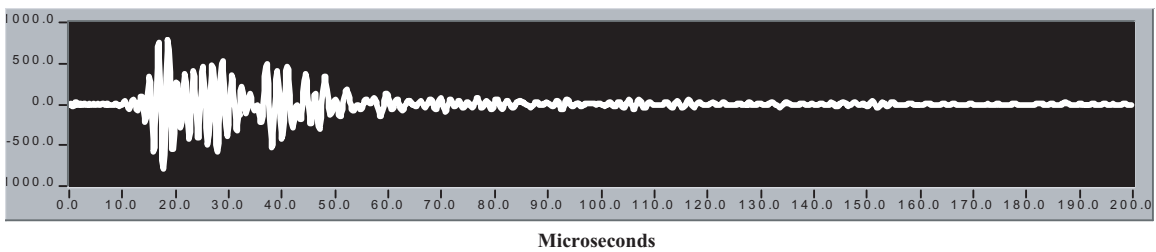
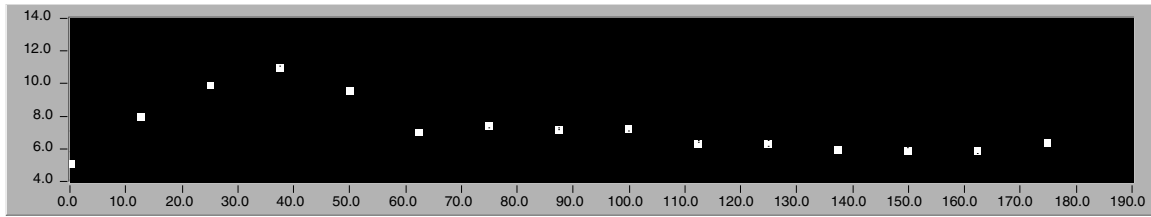
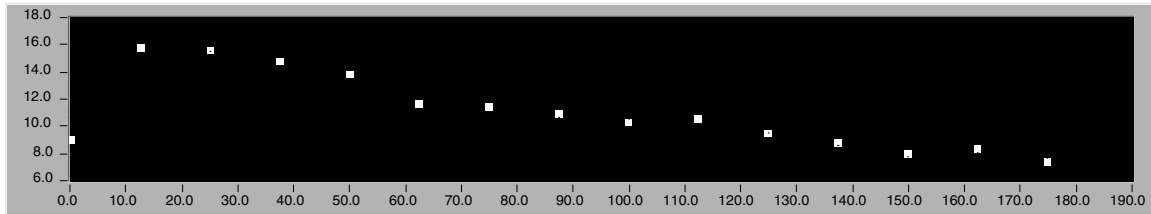


Figure 21.—Acousto-ultrasonic signal for un-aged 20-ply, 0.75 cm thick T-650-35/PMR-15 specimen PC5.

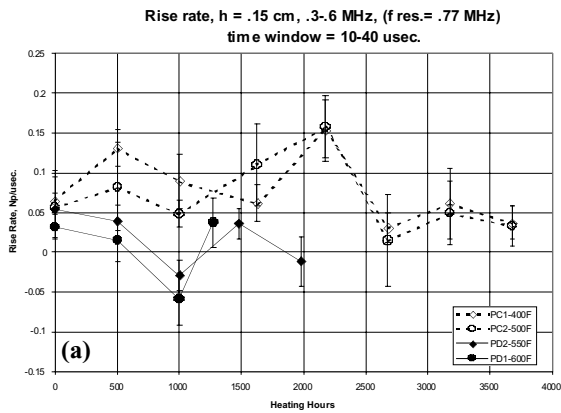


(a)

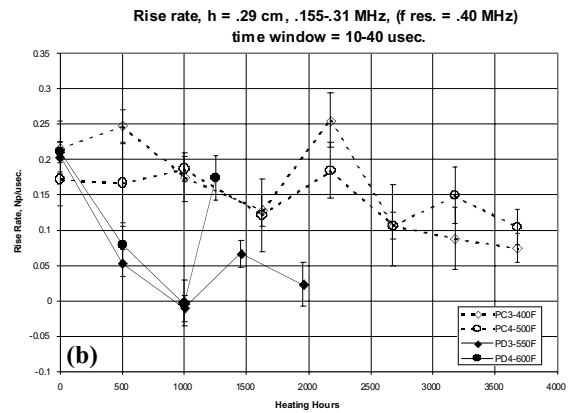


(b)

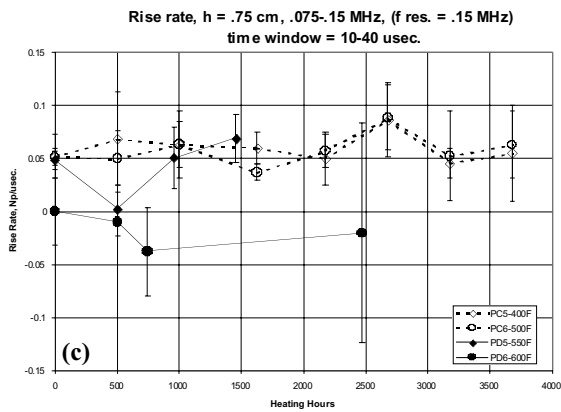
Figure 22.—Ultrasonic decay for un-aged 20-ply, 0.75 cm thick T-650-35/PMR-15 specimen PC5. (a) Ultrasonic decay graph with .075 to .150 MHz filtered zero moment of the power spectrum. (b) Ultrasonic decay graph with 0.5 to 0.9 MHz filtered zero moment of the power spectrum.



(a)

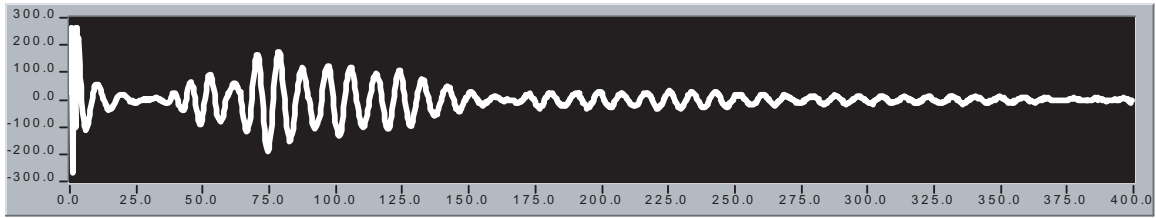


(b)

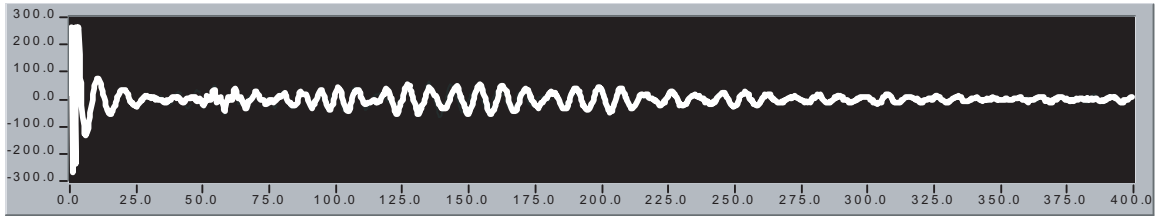


(c)

Figure 23.—Plate wave rise rates for T-650-35/PMR-15 polymer matrix composite panels.



(a)



(b)

Figure 24.—Waveforms for ultrasonic decay determination on composite fly wheel with fabrication parameters “e”. (a) Before spin test. (b) After spin test.

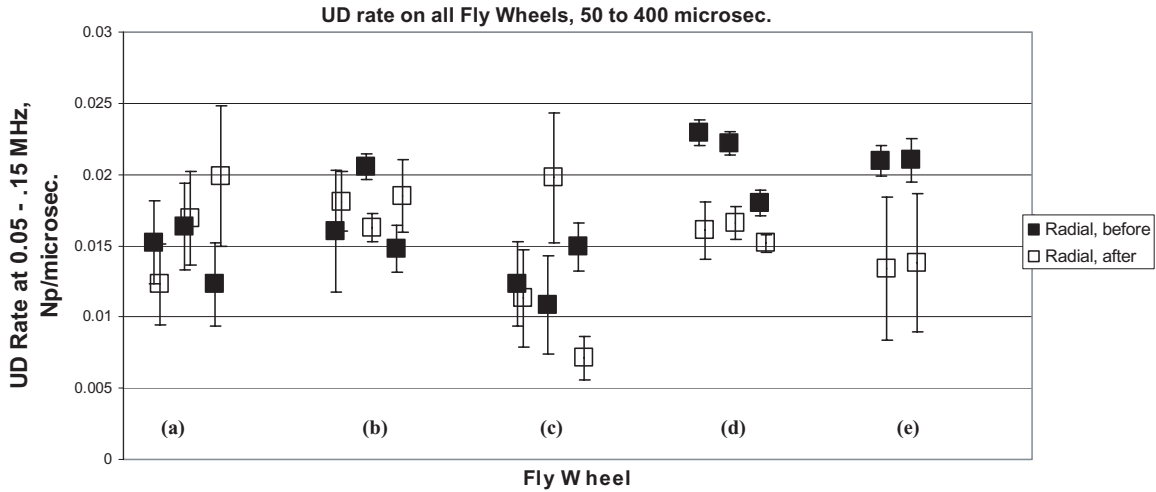


Figure 25.—Comparison of UD rates for 0.05 to .15 MHz filter for radial measurement between edge and center.

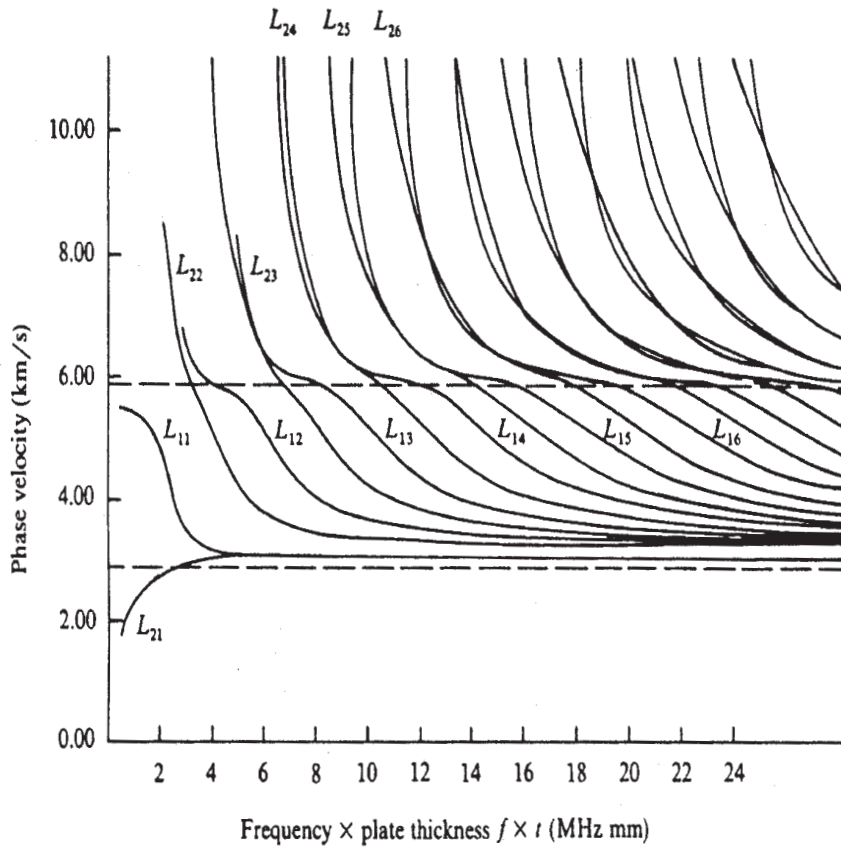


Figure A1.—Allowable plate wave modes determined by lamb.

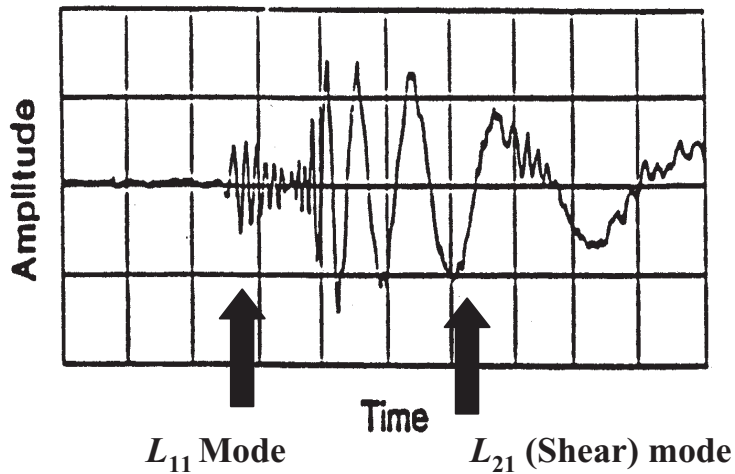


Figure A2.—Early portion of an A-U signal collected on a plate specimen.

REPORT DOCUMENTATION PAGE

Form Approved
OMB No. 0704-0188

Public reporting burden for this collection of information is estimated to average 1 hour per response, including the time for reviewing instructions, searching existing data sources, gathering and maintaining the data needed, and completing and reviewing the collection of information. Send comments regarding this burden estimate or any other aspect of this collection of information, including suggestions for reducing this burden, to Washington Headquarters Services, Directorate for Information Operations and Reports, 1215 Jefferson Davis Highway, Suite 1204, Arlington, VA 22202-4302, and to the Office of Management and Budget, Paperwork Reduction Project (0704-0188), Washington, DC 20503.

1. AGENCY USE ONLY (Leave blank)	2. REPORT DATE October 2002	3. REPORT TYPE AND DATES COVERED Final Contractor Report	
4. TITLE AND SUBTITLE Acousto-Ultrasonics to Assess Material and Structural Properties		5. FUNDING NUMBERS WU-708-73-26-00 GSN-002559	
6. AUTHOR(S) Harold E. Kautz		8. PERFORMING ORGANIZATION REPORT NUMBER E-13564	
7. PERFORMING ORGANIZATION NAME(S) AND ADDRESS(ES) Cleveland State University 1983 E. 24th Street Cleveland, Ohio 44115-2403		10. SPONSORING/MONITORING AGENCY REPORT NUMBER NASA CR-2002-211881	
9. SPONSORING/MONITORING AGENCY NAME(S) AND ADDRESS(ES) National Aeronautics and Space Administration Washington, DC 20546-0001		11. SUPPLEMENTARY NOTES Project Manager, George Y. Baaklini, Structures and Acoustics Division, NASA Glenn Research Center, organization code 5900, 216-433-6016.	
12a. DISTRIBUTION/AVAILABILITY STATEMENT Unclassified - Unlimited Subject Categories: 18, 39, 03, 26, 24, and 05 Distribution: Nonstandard Available electronically at http://gltrs.grc.nasa.gov This publication is available from the NASA Center for AeroSpace Information, 301-621-0390.		12b. DISTRIBUTION CODE	
13. ABSTRACT (Maximum 200 words) This report was created to serve as a manual for applying the Acousto-Ultrasonic NDE method, as practiced at NASA Glenn, to the study of materials and structures for a wide range of applications. Three state of the art acousto-ultrasonic (A-U) analysis parameters, ultrasonic decay (UD) rate, mean time $\langle t \rangle$ (or skewing factor, "s"), and the centroid of the power spectrum, " f_c " have been studied and applied at GRC for NDE interrogation of various materials and structures of aerospace interest. In addition to this, a unique application of Lamb wave analysis is shown. An appendix gives a brief overview of Lamb Wave analysis. This paper presents the analysis employed to calculate these parameters and the development and reasoning behind their use. It also discusses the planning of A-U measurements for materials and structures to be studied. Types of transducer coupling are discussed including contact and non-contact via laser and air. Experimental planning includes matching transducer frequency range to material and geometry of the specimen to be studied. The effect on results of initially zeroing the DC component of the ultrasonic waveform is compared with not doing so. A wide range of interrogation problems are addressed via the application of these analysis parameters to real specimens is shown for five cases: Case 1: Differences in density in [0] SiC/RBSN ceramic matrix composite. Case 2: Effect of tensile fatigue cycling in [+45] SiC/SiC ceramic matrix composite. Case 3: Detecting creep life, and failure, in Udimet 520 Nickel-Based Super Alloy. Case 4: Detecting Surface Layer Formation in T-650-35/PMR-15 Polymer Matrix Composites Panels due to Thermal Aging. Case 5: Detecting Spin Test Degradation in PMC Flywheels. Among these cases a wide range of materials and geometries are studied.			
14. SUBJECT TERMS Metal matrix composites; Signal analysis; Stress waves; Flywheels; Polymer matrix composites; Udimet alloys; Pulsed lasers; Nondestructive tests; Ceramic matrix composites; Decay rates; Gels; Frequency ranges; Lamb waves; Ultrasonics; Ultrasonic wave; Piezoelectric transducers; Attenuation; Pulse amplitude		15. NUMBER OF PAGES 48	
17. SECURITY CLASSIFICATION OF REPORT Unclassified		16. PRICE CODE	
18. SECURITY CLASSIFICATION OF THIS PAGE Unclassified	19. SECURITY CLASSIFICATION OF ABSTRACT Unclassified	20. LIMITATION OF ABSTRACT	